

**SLOVAK UNIVERSITY OF TECHNOLOGY  
IN BRATISLAVA**

**FACULTY OF CHEMICAL AND FOOD TECHNOLOGY**

Reg. No.: FCHPT-96530

# **Set-Membership State Estimation**

**MINI THESIS**

**2020**

**MSc. Carlos Eduardo Valero**



**SLOVAK UNIVERSITY OF TECHNOLOGY  
IN BRATISLAVA**

**FACULTY OF CHEMICAL AND FOOD TECHNOLOGY**

Reg. No.: FCHPT-96530

# **Set-Membership State Estimation**

**MINI THESIS**

Study programme: Process Control  
Study field: 5.2.14. Automation  
Training workspace: Institute of Information Engineering, Automation, and Mathematics  
Thesis supervisor: doc. Ing. Radoslav Paulen, PhD.

**2020**

**MSc. Carlos Eduardo Valero**



## Ing. Carlos Eduardo Valero

### Písomná práca k dizertačnej skúške

Téma dizertačnej práce:	<b>Garantovaný odhad parametrov</b>
Školiteľ:	<b>doc. Ing. Radoslav Paulen, PhD.</b>
Miesto plnenia individuálneho študijného plánu:	<b>Fakulta chemickej a potravinárskej technológie</b>
Forma štúdia:	<b>denná</b>
Začiatok štúdia:	<b>01. 09. 2018</b>
Študijný program:	<b>riadenie procesov</b>
Študijný odbor:	<b>kybernetika</b>



# Abstract

The problem of Set-membership State Estimation (SSE) is addressed. The work focuses on the main advantages and drawbacks of this kind of methodology. The theoretical background needed for developing a strategy using SSE is given (principle of convex sets theory, operation between sets and properties). Parallelotopes, and polytopes are deeply studied in the context of SSE. The most important properties and operations of the previous sets, together with their demonstrations, and also examples are given. New approaches are proposed. This is the case, for the intersection of parallelotopes, Minkowski sum, intersection and linear transformation of polytopes. A generalization of SSE approach is given taking into consideration a linear system that is found by the decomposition of a nonlinear system and various outputs signals. Moreover, two algorithms have been established to perform an SSE approach using parallelotopes or polytopes. A robust MPC control strategy is used to show the results with parallelotopes. Finally, a set of conclusions and futures challenges is given.

Keywords: Set-membership State Estimation, Set theory, Robust MPC



# Abstrakt

V tejto práci sa rieši problém odhadu stavov dynamických systémov pomocou množinovej príslušnosti (angl. Set-membership State Estimation, SSE). Práca sa zameriava na hlavné výhody a nevýhody tohto prístupu. Je uvedený teoretický základ stratégie SSE (princíp teórie konvexných množín, operácie medzi množinami a ich vlastnosti). Rovnobežníky a polytopy sú dôkladne rozobraté v kontexte SSE. Sú uvádzané najdôležitejšie vlastnosti a operácie pre tieto množiny spolu s ich ukázkami a príkladmi. Sú navrhnuté nové prístupy ako napríklad prienik rovnobežníkov, Minkowského súčet, či prienik a lineárna transformácia polytopov. Zovšeobecnenie SSE prístupu je dané s prihliadnutím na lineárny systém, ktorý je získaný rozkladom nelineárneho systému. Okrem toho sú vyvinuté dva algoritmy na vykonávanie odhadu pomocou prístupu SSE s použitím rovnobežníkov a polytopov. Na preukázanie prínosov s pomocou rovnobežníkov bola použitá robustná stratégia riadenia MPC. Na konci práce je uvedený súbor záverov a výziev do budúcnosti.

Kľúčové slová: Odhad stavu set-členstva, teória množín, robustný MPC



# Notation

## Convex Sets

$\mathcal{A}$	Convex set
$\mathcal{CZ}$	Constrained Zonotope
$\mathcal{E}$	Ellipsoid
$\mathcal{H}$	Half-space
$\mathcal{L}$	Hyperplane
$\mathcal{P}$	Parallelepiped
$\mathcal{S}$	Strip
$\mathcal{Z}$	Zonotope
$\mathbf{P}$	Polytope

$\text{conv}$  Convex hull of the set

## Real Constants and Convex Spaces

$\mathbb{R}$	Set of real numbers
$\mathbb{R}^+$	Set of positive real numbers including 0
$\mathbb{R}^n$	$n$ -dimensional real vector space
$\mathbf{0}$	$n$ dimensional constant vector of zeros
$\mathbf{0}_{no \times n}$	Matrix where all element are zero with dimension $\mathbb{R}^{no \times n}$
$\mathbf{0}_{no}$	$no$ dimensional vector of zeros
$\mathbf{1}$	$n$ -dimensional constant vector of 1
$\mathbf{A}$	State matrix of a linear system
$\mathbf{a}$	A $n$ -dimensional constant vector
$\mathbf{B}$	Input matrix of a linear system, $\mathbb{R}^{n \times n_u}$
$\mathbf{C}$	Output matrix of a linear system, $\mathbb{R}^{n \times n_o}$

---

$\mathbf{E}$	Matrix with the uncertainty relation with states in a linear systems, $\mathbb{R}^{n \times n_\omega}$
$\mathbf{F}$	Noise matrix of a linear system, $\mathbb{R}^{n_o \times n_\nu}$
$\mathbf{G}$	Facet matrix of a polytope
$\mathbf{h}$	Constant vector or offset vector of a polytope
$\mathbf{I}_{no}$	Identity matrix of dimension $no$
$\mathbf{S}$	Nonsingular matrix $\in \mathbb{R}^{n \times n}$
$\mathbf{x}$	For convex set depicts the elements of the mentioned set. In linear systems, it is known as the vector state
$\mathbf{x}_i$	Vector element of any convex set $\forall i \in \mathbb{N}$ . In linear system, it depicts the state $i$ of the vector state
$a$	Constant
$n$	Natural number
$n_\nu$	Number of independent noises in the outputs of a linear system
$n_\omega$	Number of independent uncertainties of a linear system
$n_o$	Number of state outputs of a linear system
$n_u$	Number of inputs of a linear system

# Contents

<b>Abstract</b>	<b>iii</b>
<b>Abstrakt</b>	<b>v</b>
<b>Notation</b>	<b>vii</b>
<b>List of Figures</b>	<b>xiii</b>
<b>1 Introduction</b>	<b>1</b>
<b>2 Set Theory Foundations</b>	<b>7</b>
2.1 Preliminaries . . . . .	7
2.1.1 Operations over Convex Sets . . . . .	10
2.1.2 The Conjugate Function . . . . .	10
2.2 Strips . . . . .	11
2.2.1 Definition . . . . .	11
2.2.2 Basic Operations with Strips . . . . .	12
2.3 Parallelotopes . . . . .	15
2.3.1 Definition . . . . .	15
2.3.2 Basic Operations with Parallelotopes . . . . .	16
2.3.3 Vertices of Parallelotopes . . . . .	18

2.4	Ellipsoids . . . . .	19
2.4.1	Definition . . . . .	19
2.4.2	Basic Operation with Ellipsoids . . . . .	20
2.5	Zonotopes . . . . .	21
2.5.1	Definition . . . . .	21
2.5.2	Basic Operations with Zonotopes . . . . .	21
2.6	Polytopes . . . . .	22
2.6.1	Definition . . . . .	22
2.6.2	Half-Space Representation . . . . .	22
2.6.3	Vertex Representation . . . . .	22
2.6.4	Basic Operations with Polytopes in $\mathcal{H}$ -Rep . . . . .	23
2.6.5	Geometric Problems with Polytopes . . . . .	27
<b>3</b>	<b>Set-Membership State Estimation and Control</b>	<b>29</b>
3.1	The System in Consideration . . . . .	29
3.2	Set-membership State Estimation . . . . .	31
3.2.1	Propagation . . . . .	32
3.2.2	Update . . . . .	33
3.3	Set-Membership State Estimation with Parallelotopes . . . . .	35
3.3.1	ROPO Algorithm . . . . .	36
3.3.2	ROPOe Algorithm . . . . .	38
3.3.3	Parallelotope State Estimation for Multi-output Systems . . . . .	40
3.4	Set-Membership State Estimation with Polytopes . . . . .	40
3.5	Robust MPC using SSE . . . . .	43

---

<b>4</b>	<b>Simulation Studies</b>	<b>47</b>
4.1	Case 1. SSE using Parallelotope for SISO system . . . . .	48
4.1.1	Results . . . . .	48
4.2	Case 2. SSE using Parallelotopes for SIMO system . . . . .	51
4.2.1	Results . . . . .	51
4.3	Case 3. Comparison Between Parallelotopes and Polytopes under SSE	54
4.3.1	Results . . . . .	55
4.4	Case 4. SSE using Polytopes for SISO system . . . . .	55
4.4.1	Implementation Details . . . . .	56
4.4.2	Results . . . . .	57
<b>5</b>	<b>Conclusions</b>	<b>59</b>
	<b>Bibliography</b>	<b>61</b>
	<b>Bibliography</b>	<b>61</b>



# List of Figures

2.1	Representation of a convex combination of two points. . . . .	8
2.2	Representation of the hyperplane and half-spaces in $\mathbb{R}^2$ . . . . .	9
2.3	Example of a vertex and of an edge . . . . .	9
2.4	Example of the characteristics of the strips in $\mathbb{R}^2$ . . . . .	12
2.5	Example of two half-spaces creating one strip in $\mathbb{R}^2$ . . . . .	14
2.6	Parallelotope characteristics. Example of two dimensions . . . . .	16
2.7	Example of a Chebyshev ball in a polytope of two dimensions. . . . .	28
3.1	General diagram of a set-membership state estimation approach . . . . .	31
3.2	The propagation step. . . . .	32
3.3	Example in $\mathbb{R}^2$ of the update step in a general SSE. . . . .	34
3.4	Illustration of the ROPO algorithm in a two-dimensional state space. . . . .	36
3.5	Robust MPC using set-membership state estimation. . . . .	44
4.1	Bounds on $x_1$ (top), closed-loop evolution of $x_1$ (middle), and $x_2$ (bottom). . . . .	49

4.2	Cumulative performance of min-max MPC . . . . .	50
4.3	Evolution of state variables and control input . . . . .	52
4.4	Evolution of state bounds . . . . .	53
4.5	Boxplots with statistics . . . . .	54
4.6	Polytopic and parallelotopic estimations. . . . .	56
4.7	Polytopic estimates found for 50 time steps. . . . .	57
4.8	Evolution of states, bounds and Chebyshev center . . . . .	58

# Introduction

---

Nowadays, industries strive to tackle uncertainty present in the daily business to avoid losses and to improve production performance. These uncertainties come from mismatches of the model (called uncertainties of the process) and from the inaccuracies of sensors (noises in the measurement output). The principle of robustness is used in control theory for establishing insensitivity to disturbance variation. The robustness can be reached by guaranteeing that the implemented controller steers the plant to obey the production and safety constraints. One of the ways to approach the problem is by an identification procedure that infers the values of state variables of the plant and disturbances from the available measurement outputs. A well-founded identification process under a robust control strategy will avoid constraint violation and, at the same time, will enhance the performance of the closed-loop system [17].

There are two general approaches, the probabilistic, where the algorithm requires strong assumptions on the statistical distribution of measurement noise and disturbances. This is the case of methods such as the well-known Kalman Filter (KF), which is also known as the optimal linear quadratic estimator (LQE) and deterministic approaches, such as Set-membership State Estimation (SSE), where it does not require any consideration about the probability distribution of the noise in the measurements, as well as, in the process uncertainties [8]. It is the latter approach where we want to focus. Usually, the accuracy and the complexity of the set chosen to depict the uncertainties in the SSE are inversely proportional, Le et al. [19]. Therefore, it is important to establish a trade-off between these. Even though SSE has been studied since 1970, the resulting sets there has still an arbitrary high complexity for non-conservative solutions. Moreover, the complexity rises continuously as more output data are used. In this work, it is not our intention to solve this problem, nonetheless, our contribution lies in bringing up new strategies to reduce the complexity generated for SSE approaches.

Overall, SSE methods are based on the construction of a compact set that includes, with guarantee, the states of the system that are consistent with the measured output

and take into account the bounded noise. The only consideration taken is norm-bounded uncertainty. This method splits into two important steps. The propagation step, where the chosen set is transformed accordingly to the dynamics system and the uncertainties bounds on the states. On the other side, the update step concerns about to compute the intersection of the propagated set with the output set ( A set that is created by the measurement output and the outputs bounds). Therefore, SSE approaches vary depending on the chosen set or how to perform the update step. Next paragraphs show remarkable works, in chronological order of SSE using ellipsoids, polytopes, parallelotopes, zonotopes, constrained zonotopes or a mixture of sets.

In Bertsekas and Rhodes [7], an ellipsoidal bounding approach was proposed. In this work, the authors addressed the problem of estimating the state of a linear dynamic system from noisy measurements of the output only, taking energy constraints in the output. The resulting estimator was similar in structure and comparable in simplicity to LQE. This kind of set has been studied by many authors, see, for example, [18], [10] and [22].

Kuntsevich [17] developed two strategies using polytopes or ellipsoids. The author computed the exact intersection of sets although with a high computational cost associated, Spathopoulos and Grobov [28] developed an SSE using polytopes, this time reducing the computational cost using Linear Programming (LP). However, the computational cost resulted still high in contrast with other approaches. Therefore, polytopes were in general discarded for identification processes and/or control structures due to their inherent high computational cost and complexity of the equations. Later, many researchers began using this set in combination with others to increase accuracy and reduce computational cost. This is the case for instance of [4].

Vicino and Zappa [31] developed a new SSE model using parallelotopes. The authors developed an algorithm to compute an optimal reachable parallelotope based on the minimum volume. New breakthroughs in this sense are presented by [27], where the authors use information from the past, such as Chisci et al. [11] to improve the estimation.

Zonotopes are closed under linear transformations and Minkowski sum, therefore have been used for SSE by many authors, Combastel [12] is one of the pioneers, it follows by Girard [14] and Alamo et al. [1]. These authors designed similar structures only different in the way they reduce the order of the resulting zonotope. However, these three approaches imply a significant wrapping effect, because they took the interval hull for reducing the order. Althoff et al. [4] proposed a new method for zonotope order reduction based on linear transformations that can exhibit better overapproximations

---

than the previous approaches.

Scott et al. [26] introduced a new class of sets, called constrained zonotopes, that can be used to enclose sets of interest for estimation and control. The resulting set is able to depict any arbitrary polytope. Because of this, it is called a new representation of polytopes, however, it implies in high order representation, even for polytopes with few half-spaces. The biggest advantage of constrained zonotopes lies in that they are closed under many operations (Minkowski sum, intersection, linear transformation, and projections) which brings simple SSE formulations. This approach has gained acknowledgment and there are many authors working in this area, for instance [24].

Overall, the SSE is well studied but still has many open problems. The implementation of different sets brings some advantages over others. Convex sets for estimation and control have been studied since 1970. Thus, many tools can be found to perform estimation and control in a relatively simple way.

The Multi-Parametric Toolbox (MPT) by [15] is a collection of algorithms that features a powerful geometric library where a great variety of set-membership control and identification problems can be solved. At the same time, it can be used for modeling, control, analysis, and deployment of constrained optimal controllers.

The COntinuous Reachability Analyzer (CORA) developed by [3] is a toolbox that integrates various set representations and operations on them as well as reachability algorithms of various dynamic system classes. It is specifically designed to work with set-membership problems, although, it can be used for other purposes.

Despite these tools and differences approaches, the perfect solution is far from being achieved. The non-conservative solution for system controlling or system identification and/or estimation is still arbitrarily complex and rises while more data is collected. Therefore, the main goal of this research focuses on developing a new approach for set-membership state estimation together with one suitable control structure and to bring a researcher handbook for set-membership in control.

## Motivation

The main motivation of research in the SSE approach lies in improving current methodologies in parallelotopes, polytopes, and zonotopes. Past measurement outputs can be taken to reduce the feasibility set in many approaches, a clever method to select particular measurement outputs from the past is required (In this work, we suggest

one for parallelotope state estimation). Another way to enhance the performance of SSE, it is finding new algorithms that reduce the complexity of the sets used. In this context, a new necessary and sufficient condition to compute the Minkowski sum in polytopes is required (a necessary, but do not sufficient condition is proposed) and a unique optimization problem to computed an SSE is also needed. Furthermore, the zonotope order reduction problem is still open in the research area. New ideas suggest that a transformation matrix could lead to less conservative sets. However, the way to select the transformation matrix is not clear. We believe that a rotation matrix is a key to find the minimum order zonotope that encloses the higher zonotope.

## General Objectives

The main goal of our work is to bring up three new approaches to tackle Set-membership State Estimation. In this sense, we can summarize the objectives in the following way,

- Develop a new Set-membership State Estimation using Parallelotopes taking information from the past.
- Develop a new Set-membership State Estimation using Polytopes throughout one single non-linear problem.
- Develop a Set-membership State Estimation using zonotopes with a new zonotope order reduction technique.

As a consequence of these objectives, it is expected:

- Build up a complete review of the current methods for SSE for every set (polytopes, ellipsoids, parallelotopes, zonotopes, constrained zonotopes).
- Establish a researcher handbook for SSE that includes the minimum mathematical requirements, methods, algorithms, and examples for a variety of systems with the aim to encourage new researchers with a well-defined path.
- Formulate new necessary and sufficient conditions for Minkowski sum of polytopes.
- Build up new zonotope properties and operations.

## Publications

Content of this thesis is primarily based on the following publications,

- Valero, C. E., Villanueva, M. E., Houska B., & Paulen, R. (2020). **Set-Based State Estimation: A Polytopic Approach**. IFAC World Congress, Accepted.
- Valero, C. E., & Paulen, R. (2019). **Set-Theoretic State Estimation for Multi-output Systems using Block and Sequential Approaches**. In 2019 22nd International Conference on Process Control (PC19) (pp. 268-273). IEEE.
- Valero, C. E., & Paulen, R. (2019). **Effective Recursive Set-membership State Estimation for Robust Linear MPC**. DYCOPS Conference, IFAC-Papers OnLine, 52(1), 486-491.



# Set Theory Foundations

---

In this chapter, the mathematical foundations about convex sets that are going to be used in this work are presented.

## 2.1 Preliminaries

Before presenting the most well-known families of convex sets, some basic definitions and operations are required. Thus, this section has the purpose of clarifying to the reader some essential notions about convex sets which will be useful further. [9] and [8] are good references for more details.

**Definition 1** (Linear Combination). *Given  $n$  vectors  $\{\mathbf{x}_1, \mathbf{x}_2, \dots, \mathbf{x}_n\}$  and  $n$  constants  $\{a_1, a_2, \dots, a_n\}$ , the linear combination of the vectors is given by,*

$$\sum_{i=1}^n a_i \mathbf{x}_i \quad (2.1)$$

where  $a_i \in \mathbb{R}$  is the only condition.

**Definition 2** (Convex Combination). *Given  $n$  vectors  $\{\mathbf{x}_1, \mathbf{x}_2, \dots, \mathbf{x}_n\}$  and  $n$  constants  $\{\alpha_1, \alpha_2, \dots, \alpha_n\}$ , the convex combination of the vectors is given by,*

$$\sum_{i=1}^n \alpha_i \mathbf{x}_i \quad (2.2)$$

where  $\alpha_i \in \mathbb{R}^+$  and  $\sum_{i=1}^n \alpha_i = 1$ .

The convex combination of two points  $\mathbf{x}_1$  and  $\mathbf{x}_2$  can be described by  $\alpha \mathbf{x}_1 + (1 - \alpha) \mathbf{x}_2$ , where,  $0 \leq \alpha \leq 1$ . From a geometrical point of view, the convex combination between

two points is the line drawn between  $\mathbf{x}_1$  and  $\mathbf{x}_2$ . In Figure 2.1 the line of points that depicts this situation is drawn.

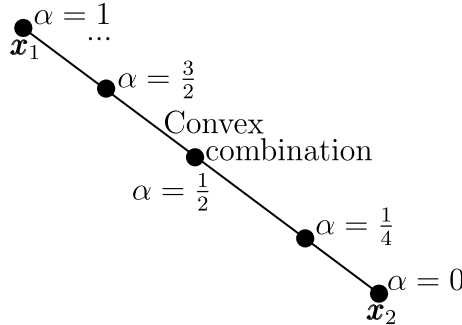


**Figure 2.1:** Representation of a convex combination of two points.

**Definition 3** (Convex Set). A set  $\mathcal{C} \subset \mathbb{R}^n$  is convex, if and only if

$$\forall \mathbf{x}_1, \mathbf{x}_2 \in \mathcal{C}, \alpha \mathbf{x}_1 + (1 - \alpha) \mathbf{x}_2 \in \mathcal{C} \quad (2.3)$$

where  $\alpha \in \mathbb{R}$  with  $0 \leq \alpha \leq 1$ . Equivalently, a set  $\mathcal{C}$  is convex if and only if for each pair of distinct points  $\mathbf{x}_1, \mathbf{x}_2 \in \mathcal{C}$  the closed segment with endpoints  $\mathbf{x}_1$  and  $\mathbf{x}_2$  is contained in  $\mathcal{C}$ .

**Definition 4** (Convex Hull). The **convex hull** (conv) of a set  $\mathcal{C} \in \mathbb{R}^n$  is the intersection of all possible convex set, that contain  $\mathcal{C}$ . It is the set of all points which may be depicted as convex combinations of points of  $\mathcal{C}$ .

**Definition 5** (Hyperplane and Half-Space). A **hyperplane**  $\mathcal{L}$  is a set which may be defined as  $\mathcal{L}(\mathbf{g}, h) = \{\mathbf{x} \in \mathbb{R}^n \mid \mathbf{g}^\top \mathbf{x} = h\}$ , where  $\mathbf{g} \neq \mathbf{0}$  and  $h \in \mathbb{R}$ . Geometrically,  $\mathbf{g}$  is the normal vector of the hyperplane  $\mathcal{L}$  and  $h$  determines the offset of the hyperplane from the origin. A closed **half-space**  $\mathcal{H}(\mathbf{g}, h)$  is defined as  $\{\mathbf{x} \in \mathbb{R}^n \mid \mathbf{g}^\top \mathbf{x} \leq h\}$  for  $\mathbf{g} \neq \mathbf{0}$ . In Figure 2.2, both concepts are illustrated.

**Definition 6** (Polyhedron). A set  $\mathcal{C} \subset \mathbb{R}^n$  is a polyhedron, if and only if, the set is the intersection of  $m$  half-spaces. Clearly, a half-space itself is a polyhedron.

**Definition 7** (The Minimal Representation). A linear inequality  $\mathbf{a}^\top \mathbf{x} \leq b$  is called valid for a polyhedron  $\mathcal{C}$ , if and only if  $\mathbf{a}^\top \mathbf{x} \leq b$  holds  $\forall \mathbf{x} \in \mathcal{C}$ . Therefore, a polyhedron can have infinite valid half-spaces and can be represented by many redundant half-spaces. The polyhedron with the minimum number of half-spaces that depict it is called **the minimal representation**.

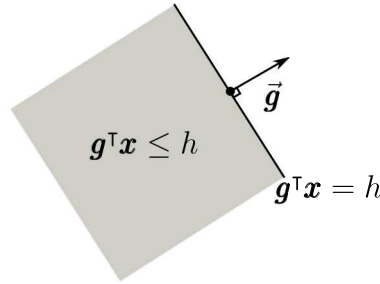


**Figure 2.2:** Representation of the hyperplane and half-spaces in  $\mathbb{R}^2$ .

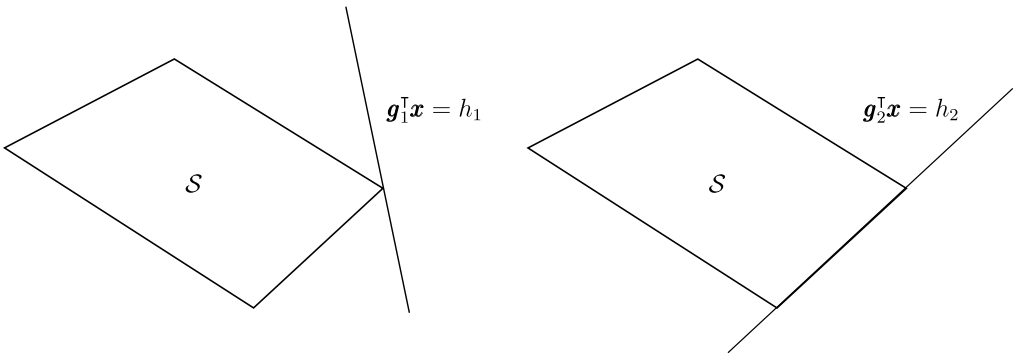


**Figure 2.3:** Example of a vertex (left-hand plot) and of an edge (right-hand plot), respectively in  $\mathbb{R}^2$ .

**Definition 8** (Faces, Vertices, Edges, Ridges, and Facets). *A subset of a polyhedron  $\mathcal{C}$  is called a face of  $\mathcal{C}$  if it can be represented as*

$$\mathcal{F} = \mathcal{C} \cap \{\mathbf{x} \in \mathbb{R}^n \mid \mathbf{a}^\top \mathbf{x} = b\} \quad (2.4)$$

*The dimension of a face is the number of variables needed to describe  $\mathcal{F}$  uniquely for some valid inequality. The faces of a polyhedron  $\mathcal{C}$  of dimensions  $0, 1, \dots, (n-2)$ , and  $(n-1)$  are called vertices, edges, ridges, and facets, respectively. The Figure 2.3 shows two valid inequalities for a polyhedron in  $\mathbb{R}^2$ , i.e., a vertex and an edge.*

**Definition 9** (Supporting hyperplane). *Denote  $\mathcal{C} \subset \mathbb{R}^n$  an arbitrary convex set. Then, the hyperplane,*

$$\mathcal{L}(\mathbf{g}, h) = \{\mathbf{x} \in \mathbb{R}^n \mid \mathbf{g}^\top \mathbf{x} = h\} \quad (2.5)$$

*is a **supporting** or tangent hyperplane for  $\mathcal{C}$ , if and only if,  $\mathbf{g}^\top \mathbf{x} \geq h$  or  $\mathbf{g}^\top \mathbf{x} \leq h$ ,  $\forall \mathbf{x} \in \mathcal{C}$ . One way to find a supporting hyperplane is through the support function, the*

function  $\sigma[\mathcal{C}](\mathbf{g})$  defined as,

$$\sigma[\mathcal{C}](\mathbf{g}) = \max_{\mathbf{x} \in \mathcal{C}} \mathbf{g}^\top \mathbf{x} \quad (2.6)$$

is said to be the support function. A convex and closed set can be represented in terms of its support function. If  $\mathcal{C}$  is a convex and closed set, then

$$\mathcal{C} = \{\mathbf{x} \in \mathbb{R}^n \mid \mathbf{g}^\top \mathbf{x} = \sigma(\mathcal{C})\} \quad \forall \mathbf{g} \in \mathbb{R}^n \quad (2.7)$$

## 2.1.1 Operations over Convex Sets

We present some basic operations over sets, which will become useful below. Let  $\mathcal{A}$  and  $\mathcal{B}$  be any convex sets, and let  $\lambda \in \mathbb{R}$ .

### 2.1.1.1 Minkowski Sum

The Minkowski sum of two sets is given by,

$$\mathcal{A} \oplus \mathcal{B} = \{\mathbf{a} + \mathbf{b}, \quad \forall \mathbf{a} \in \mathcal{A}, \forall \mathbf{b} \in \mathcal{B}\} \quad (2.8)$$

### 2.1.1.2 Scaling

$$\lambda \mathcal{A} = \{\lambda \mathbf{a}, \quad \forall \mathbf{a} \in \mathcal{A}\} \quad (2.9)$$

### 2.1.1.3 Intersection

The intersection of two sets is given by,

$$\mathcal{A} \cap \mathcal{B} = \{\mathbf{x} \mid \mathbf{x} \in \mathcal{A}, \mathbf{x} \in \mathcal{B}\} \quad (2.10)$$

## 2.1.2 The Conjugate Function

The conjugate function will allow to demonstrate some useful properties. It is the key to duality problems in optimization. The conjugate function is defined as

$$f^*(\mathbf{y}) = \sup_{\mathbf{x} \in \text{dom } f} (\mathbf{y}^\top \mathbf{x} - f(\mathbf{x})) \quad (2.11)$$

where the function  $f^* : \mathbb{R}^n \rightarrow \mathbb{R}$  and  $\text{dom}$  depicts the domain of a function. The domain of the conjugate function consists of  $\mathbf{y} \in \mathbb{R}^n$  for which the supremum is finite. This is, for which the difference  $\mathbf{y}^\top \mathbf{x} - f(\mathbf{x})$  is bounded above on  $\text{dom } f$ . The conjugate function,  $f^*$  is always a convex function since it is the pointwise supremum of a family of convex functions of  $\mathbf{y}$ . This is true whether or not  $f$  is convex. The following example will clarify the definition and it will help in the future.

**Example 1** (The affine function).  $f(\mathbf{x}) = \mathbf{a}^\top \mathbf{x} + b$ . As a function of  $\mathbf{x}$ ,  $\mathbf{y}^\top \mathbf{x} - \mathbf{a}^\top \mathbf{x} - b$  is bounded if and only if  $\mathbf{y} = \mathbf{a}$ , in which case, it is constant. Therefore the domain of the conjugate function  $f^*$  is the constant vector  $\mathbf{a}$ , and  $f^*(\mathbf{a}) = -b$ .

## 2.2 Strips

Strips are unbounded sets, built up with two parallel half-spaces. Strips are only closed under linear transformations and they are not used as set for estimation at least not in a direct way.

### 2.2.1 Definition

Given an arbitrary non-zero vector  $\mathbf{p}$  and a real constant  $c$ , a *strip* is an unbounded set of points that satisfy:

$$\mathcal{S}(\mathbf{p}, c) := \{\mathbf{x} \mid \mathbf{p}^\top \mathbf{x} - c \leq 1\} \quad (2.12)$$

where  $\mathbf{p} \in \mathbb{R}^n$  and  $c \in \mathbb{R}$ . Its supporting hyperplanes are given by,

$$\mathcal{H}^+ = \{\mathbf{x} \in \mathbb{R}^n \mid \mathbf{p}^\top \mathbf{x} = c + 1\} \quad (2.13)$$

$$\mathcal{H}^- = \{\mathbf{x} \in \mathbb{R}^n \mid \mathbf{p}^\top \mathbf{x} = c - 1\} \quad (2.14)$$

**Remark 1.** Given two strips  $\mathcal{S}_1(\mathbf{p}_1, c_1)$  and  $\mathcal{S}_2(\mathbf{p}_2, c_2)$ ,  $\mathcal{S}_1$  is contained in  $\mathcal{S}_2$  ( $\mathcal{S}_1(\mathbf{p}_1, c_1) \subseteq \mathcal{S}_2(\mathbf{p}_2, c_2)$ ), if and only if,  $\exists \lambda, 0 < \lambda \leq 1$ , such that

$$\mathbf{p}_2 = \lambda \mathbf{p}_1 \quad (2.15)$$

$$|c_2 - \lambda c_1| \leq 1 - \lambda \quad (2.16)$$

**Definition 10.** The strip  $\mathcal{S}(\mathbf{p}, c)$  is said to be tight with respect to  $\mathcal{C}$  if both  $\mathcal{H}^+$  and  $\mathcal{H}^-$  are supporting hyperplanes for  $\mathcal{C}$ .

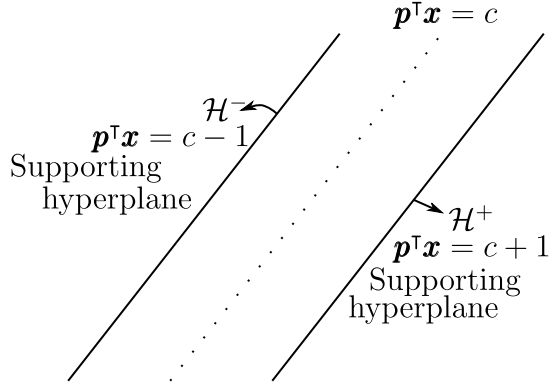


Figure 2.4: Example of the characteristics of the strips in  $\mathbb{R}^2$ .

## 2.2.2 Basic Operations with Strips

### 2.2.2.1 Linear Transformation

Given strips  $\mathcal{S}_1(\mathbf{p}_1, c_1)$  and  $\mathcal{S}_2(\mathbf{p}_2, c_2)$ , it is said that  $\mathcal{S}_2(\mathbf{p}_2, c_2)$  is a linear transformation of  $\mathcal{S}_1(\mathbf{p}_1, c_1)$ , if and only if, there exists a nonsingular matrix  $\mathbf{S} \in \mathbb{R}^{n \times n}$  and a linear relation  $\mathbf{x}_2 = \mathbf{S}\mathbf{x}_1 + \mathbf{a}$  with  $\mathbf{a} \in \mathbb{R}^{n \times 1}$ , where,

$$\mathbf{p}_2 := \mathbf{p}_1^T \mathbf{S}^{-1}, \quad c_2 := c_1 + \mathbf{p}_1^T \mathbf{S}^{-1} \mathbf{a}. \quad (2.17)$$

**Proof 1.**

$$\mathbf{x}_2 = \mathbf{S}\mathbf{x}_1 + \mathbf{a} \quad (2.18)$$

$$\mathbf{x}_2 - \mathbf{a} = \mathbf{S}\mathbf{x}_1 \quad (2.19)$$

$$\mathbf{x}_1 = \mathbf{S}^{-1}(\mathbf{x}_2 - \mathbf{a}) \quad (2.20)$$

$$\mathbf{x}_1 = \mathbf{S}^{-1}\mathbf{x}_2 - \mathbf{S}^{-1}\mathbf{a} \quad (2.21)$$

Using a substitution of  $\mathbf{x}_1$  into strip definition, it results in

$$\mathcal{S}_1(\mathbf{p}_1, c_1) = \{\mathbf{x}_1 : |\mathbf{p}_1^T \mathbf{x}_1 - c_1| \leq 1\} \quad (2.22)$$

$$\Rightarrow \{\mathbf{x}_2 : |\mathbf{p}_1^T (\mathbf{S}^{-1}\mathbf{x}_2 - \mathbf{S}^{-1}\mathbf{a}) - c_1| \leq 1\} \quad (2.23)$$

$$= \{\mathbf{x}_2 : |\mathbf{p}_1^T \mathbf{S}^{-1}\mathbf{x}_2 - \mathbf{p}_1^T \mathbf{S}^{-1}\mathbf{a} - c_1| \leq 1\} \quad (2.24)$$

### 2.2.2.2 Developing Strips from Half-spaces

The supporting hyperplanes ( $\mathcal{H}^-$  and  $\mathcal{H}^+$ ) and the center hyperplane are depicted in Figure 2.4 (one strip with its supporting hyperplanes). Thus, it is evident that any

strip can be represented as a non-void intersection of two parallel half-spaces. In this sense, it is said that two half-spaces,  $\mathcal{H}_1(\mathbf{g}_1, h_1)$  and  $\mathcal{H}_2(\mathbf{g}_2, h_2)$  are parallel if and only if,  $\exists \alpha \in \mathbb{R}$ , such that  $\mathbf{g}_1 = \alpha \mathbf{g}_2$ . This means, it is possible to write both,  $\mathcal{H}_1$  and  $\mathcal{H}_2$ , in the following manner,

$$h_1 \leq \mathbf{g}_1^\top \mathbf{x} \leq \alpha h_2$$

The next step is to find a real value to add to the inequalities such that the absolute value of the constant terms in both sides is the same. This can be solved if we propose a system of two equations with two variables, where  $a \in \mathbb{R}$  will be the constant to add in the inequalities and  $b \in \mathbb{R}$  the desired value. This is,

$$h_1 + a = -b \quad (2.25)$$

$$\alpha h_2 + a = b \quad (2.26)$$

$$\Rightarrow a = -\frac{h_1 + \alpha h_2}{2} \quad (2.27)$$

Thus

$$h_1 - \frac{h_1 + \alpha h_2}{2} \leq \mathbf{g}_1^\top \mathbf{x} - \frac{h_1 + \alpha h_2}{2} \leq h_2 - \frac{h_1 + \alpha h_2}{2} \quad (2.28)$$

$$-\frac{h_1 - \alpha h_2}{2} \leq \mathbf{g}_1^\top \mathbf{x} - \frac{h_1 + \alpha h_2}{2} \leq \frac{h_1 - \alpha h_2}{2} \quad (2.29)$$

$$-1 \leq \frac{2}{h_1 - \alpha h_2} \mathbf{g}_1^\top \mathbf{x} - \frac{h_1 + \alpha h_2}{h_1 - \alpha h_2} \leq 1 \quad (2.30)$$

The resulting inequalities represent a strip  $\mathcal{S}(\mathbf{p}, c)$  where  $\mathbf{p} = \frac{2}{h_1 - \alpha h_2} \mathbf{g}_1$  and  $c = \frac{h_1 + \alpha h_2}{h_1 - \alpha h_2}$ .

**Example 2.** Given two parallel half-spaces of the form (See Figure 2.5),

$$\begin{bmatrix} 1 & 1 \end{bmatrix} \begin{bmatrix} \mathbf{x}_1 \\ \mathbf{x}_2 \end{bmatrix} \leq 5, \quad \begin{bmatrix} -2 & -2 \end{bmatrix} \begin{bmatrix} \mathbf{x}_1 \\ \mathbf{x}_2 \end{bmatrix} \leq -6 \quad (2.31)$$

The strip associated with the half-spaces is given by,

$$\left\{ \mathbf{x} \in \mathbb{R}^2 \mid \begin{bmatrix} -1 & -1 \end{bmatrix} \begin{bmatrix} \mathbf{x}_1 \\ \mathbf{x}_2 \end{bmatrix} + 4 \leq 1 \right\} \quad (2.32)$$

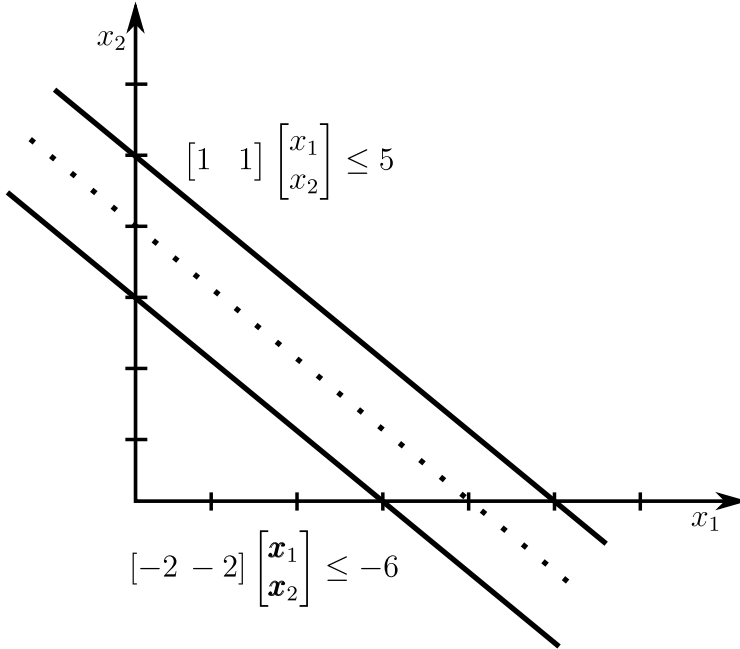


**Figure 2.5:** Example of two half-spaces creating one strip in  $\mathbb{R}^2$ .

**Example 3** (Strips from Linear Systems). *we consider a discrete-time linear single output system under a bounded perturbation that can be expressed in the time step  $k$  such as,*

$$y_{m,k} = \mathbf{C}\mathbf{x}_k \pm \varepsilon_k$$

where  $\varepsilon_k \in [-\varepsilon, \varepsilon]$  depicts the bounded error,  $\mathbf{x}_k \in \mathbb{R}^n$  is the system state vector at time step  $k$ ,  $\mathbf{C} \in \mathbb{R}^{1 \times n}$  is the output matrix (vector in this case), and  $y_{m,k} \in \mathbb{R}$  is the measurement output. It is clear that the error between the measurement output and the linear system is given by,

$$-\varepsilon \leq \mathbf{C}\mathbf{x}_k - y_{m,k} \leq \varepsilon$$

Now, if we compare this equation with (2.29), the strip for the linear system is given by,

$$\left| \frac{\mathbf{C}}{\varepsilon}\mathbf{x}_k - \frac{y_{m,k}}{\varepsilon} \right| \leq 1 \quad (2.33)$$

## 2.3 Parallelotopes

This section summarizes the most important properties and operations of parallelotopes that are going to be useful in this work.

### 2.3.1 Definition

A parallelotope can be defined in terms of half-spaces, such as a nonvoid intersection of  $2n$  parallel half-spaces. In terms of polyhedrons, it is a bounded, symmetric polyhedron with facet matrix  $\mathbf{G} \in \mathbb{R}^{2n \times n}$ . In terms of polytopes, it is a symmetric polytope with facet matrix  $\mathbf{G} \in \mathbb{R}^{2n \times n}$ . In terms of strips, it is a non-empty bounded intersection of  $n$  strips. All definitions are valid and equivalent and can be useful depending on the case to demonstrate or to compute particular operations.

A mathematical way to define a parallelotope is given,

$$\mathcal{P} = \bigcap_{i=1}^n \mathcal{S}(\mathbf{p}_i, c_i) \quad (2.34)$$

Which is equivalent to,

$$\mathcal{P} = \{\mathbf{x} \in \mathbb{R}^n \mid \|\mathbf{P}\mathbf{x} - \mathbf{c}\|_\infty \leq 1\} \quad (2.35)$$

where  $\mathbf{P} \in \mathbb{R}^{n \times n}$  and  $\mathbf{c} \in \mathbb{R}^{n \times 1}$ . If the intersection of strips is bounded and nonempty, the inverse of  $\mathbf{P}$  exists. Thus, applying a change of variables as  $\mathbf{v} = \mathbf{P}\mathbf{x} - \mathbf{c}$ , defining  $\mathbf{T} = \mathbf{P}^{-1}$ ,  $\boldsymbol{\theta}_c = \mathbf{T}\mathbf{c}$ , equation (2.35) turns into,

$$\mathcal{P}(\mathbf{T}, \boldsymbol{\theta}_c) = \{\mathbf{x} = \mathbf{T}\mathbf{v} + \boldsymbol{\theta}_c, \|\mathbf{v}\|_\infty \leq \mathbf{1}\} \quad (2.36)$$

This new equation is known as the generator form. Clearly  $\mathbf{v}$  is limited by the unit square of  $\mathbb{R}^n$ . Thus, the columns of  $\mathbf{T} = [\mathbf{t}_1 \ \mathbf{t}_2 \ \dots \ \mathbf{t}_n]$  determine the size and shape of the parallelotope that is going to be placed around  $\boldsymbol{\theta}_c$ . For this reason,  $\mathbf{T}$  is called the generator matrix and  $\boldsymbol{\theta}_c$  the center of a parallelotope. An example of a parallelotope in  $\mathbb{R}^2$  is shown in Figure 2.6.

The  $\mathcal{H}$ -rep of a parallelotope can be deduced from (2.35), understanding that parallelotopes have  $2n$  facets where  $n$  of them are non-parallel, and each of the rows of  $\mathbf{P}$  describes the direction of each half-space. Therefore

$$\mathcal{P}(\mathbf{G}_p, \mathbf{h}_p) = \left\{ \mathbf{x} \in \mathbb{R}^n \mid \begin{bmatrix} \mathbf{P} \\ -\mathbf{P} \end{bmatrix} \mathbf{x} \leq \begin{bmatrix} \mathbf{1} + \mathbf{c} \\ \mathbf{1} - \mathbf{c} \end{bmatrix} \right\} \quad (2.37)$$

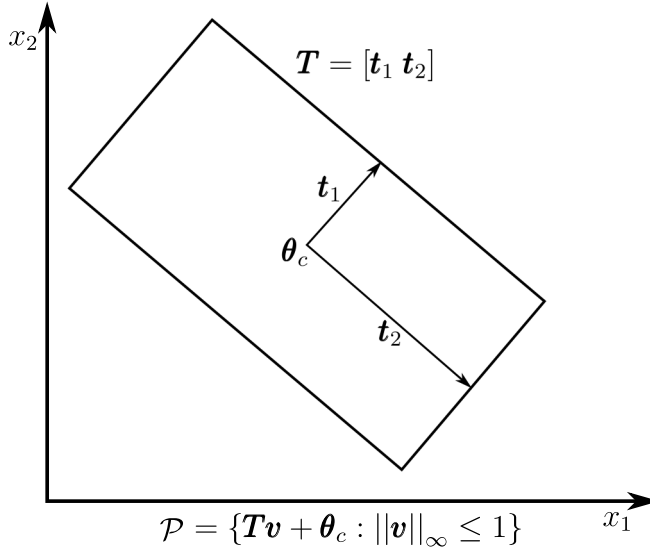


Figure 2.6: Paralleloptope characteristics. Example of two dimensions

## 2.3.2 Basic Operations with Parallelotopes

### 2.3.2.1 Linear Transformation

Given parallelotopes  $\mathcal{P}_1(\mathbf{T}_1, \boldsymbol{\theta}_{c,1})$  and  $\mathcal{P}_2(\mathbf{T}_2, \boldsymbol{\theta}_{c,2})$ , it is said that  $\mathcal{P}_2(\mathbf{T}_2, \boldsymbol{\theta}_{c,2})$  is a linear transformation of  $\mathcal{P}_1(\mathbf{T}_1, \boldsymbol{\theta}_{c,1})$  if and only if, exists a nonsingular matrix  $\mathbf{S} \in \mathbb{R}^{n \times n}$  and a linear relation  $\mathbf{x}_2 = \mathbf{S}\mathbf{x}_1 + \mathbf{q}$  with  $\mathbf{q} \in \mathbb{R}^{n \times 1}$ . Therefore,

$$\mathbf{T}_2 = \mathbf{S}\mathbf{T}_1 \quad \boldsymbol{\theta}_{c,2} = \mathbf{S}\boldsymbol{\theta}_{c,1} + \mathbf{q} \quad (2.38)$$

**Proof 2.**

$$\mathbf{x}_2 = \mathbf{S}\mathbf{x}_1 + \mathbf{q} \quad (2.39)$$

$$\mathbf{x}_2 = \mathbf{S}(\mathbf{T}_1\mathbf{v}_1 + \boldsymbol{\theta}_{c,1}) + \mathbf{q}, \|\mathbf{v}_1\|_\infty \leq 1 \quad (2.40)$$

$$\mathbf{x}_2 = \mathbf{S}\mathbf{T}_1\mathbf{v}_1 + \mathbf{S}\boldsymbol{\theta}_{c,1} + \mathbf{q}, \|\mathbf{v}_1\|_\infty \leq 1 \quad (2.41)$$

Thus, using (2.38)

$$\mathbf{x}_2 = \mathbf{T}_2\mathbf{v}_2 + \boldsymbol{\theta}_{c,2}, \|\mathbf{v}_2\|_\infty \leq 1 \quad (2.42)$$

$$(2.43)$$

### 2.3.2.2 Minkowski Sum

Parallelotopes are not closed under Minkowski sum. This means, that in general the addition of two parallelotopes is not a parallelotope. This operation is determined in the following way. Given parallelotopes  $\mathcal{P}_1(\mathbf{T}_1, \boldsymbol{\theta}_{c,1})$  and  $\mathcal{P}_2(\mathbf{T}_2, \boldsymbol{\theta}_{c,2})$ . The Minkowski sum is given by,

$$\mathbf{T}_s = [\mathbf{T}_1 \quad \mathbf{T}_2] \quad \boldsymbol{\theta}_{c,s} = \boldsymbol{\theta}_{c,1} + \boldsymbol{\theta}_{c,2} \quad (2.44)$$

Latter we will show that this expression depicts a zonotope and it can be reduced using special techniques.

### 2.3.2.3 Intersection

The intersection is another non closed operation for parallelotope. However, it is possible to find a parallelotope that encloses the intersection in a simple way. We propose the following relations. Given parallelotopes  $\mathcal{P}_1(\mathbf{T}_1, \boldsymbol{\theta}_{c,1})$  and  $\mathcal{P}_2(\mathbf{T}_2, \boldsymbol{\theta}_{c,2})$ , a parallelotope that encloses the intersection  $\mathcal{P}_\cap(\mathbf{T}_\cap, \boldsymbol{\theta}_{c,\cap})$  it is given by,

$$\begin{aligned} \mathbf{T}_\cap &= 2\mathbf{T}_1(\mathbf{T}_1 + \mathbf{T}_2)^{-1}\mathbf{T}_2 \\ \boldsymbol{\theta}_{c,\cap} &= \mathbf{T}_2(\mathbf{T}_1 + \mathbf{T}_2)^{-1}\boldsymbol{\theta}_{c,1} + \mathbf{T}_1(\mathbf{T}_1 + \mathbf{T}_2)^{-1}\boldsymbol{\theta}_{c,2} \end{aligned} \quad (2.45)$$

**Proof 3.** *By definition, the intersection of  $\mathcal{P}_1$  and  $\mathcal{P}_2$ , i.e.,  $\mathcal{P}_1 \cap \mathcal{P}_2$  represents the set of all elements  $\mathbf{x}$  that belong to  $\mathcal{P}_1$  and  $\mathcal{P}_2$ . This can be described by,*

$$\mathcal{P}_\cap = \mathbf{x} \in \mathcal{P}_1, \mathbf{x} \in \mathcal{P}_2 \quad (2.46)$$

$$\mathcal{P}_\cap = \{\mathbf{x} = \mathbf{T}_1\mathbf{v}_1 + \boldsymbol{\theta}_{c,1} : \|\mathbf{v}_1\|_\infty \leq 1\}, \{\mathbf{x} = \mathbf{T}_2\mathbf{v}_2 + \boldsymbol{\theta}_{c,2} : \|\mathbf{v}_2\|_\infty \leq 1\} \quad (2.47)$$

At the same time we know that,

$$\mathbf{v}_1 = \mathbf{T}_1^{-1}(x - \boldsymbol{\theta}_{c,1}) \quad \mathbf{v}_2 = \mathbf{T}_2^{-1}(x - \boldsymbol{\theta}_{c,2}) \quad (2.48)$$

In order to find a relation between both definitions in Equation (2.48), both conditions are added.

$$\|\mathbf{v}_1 + \mathbf{v}_2\|_\infty \leq 2 \quad (2.49)$$

$$\|\mathbf{T}_1^{-1}(x - \boldsymbol{\theta}_{c,1}) + \mathbf{T}_2^{-1}(x - \boldsymbol{\theta}_{c,2})\|_\infty \leq 2 \quad (2.50)$$

$$\|\mathbf{T}_1^{-1}x - \mathbf{T}_1^{-1}\boldsymbol{\theta}_{c,1} + \mathbf{T}_2^{-1}x - \mathbf{T}_2^{-1}\boldsymbol{\theta}_{c,2}\|_\infty \leq 2 \quad (2.51)$$

$$\|(\mathbf{T}_1^{-1} + \mathbf{T}_2^{-1})x - (\mathbf{T}_1^{-1}\boldsymbol{\theta}_{c,1} + \mathbf{T}_2^{-1}\boldsymbol{\theta}_{c,2})\|_\infty \leq 2 \quad (2.52)$$

$$\frac{\|(\mathbf{T}_1^{-1} + \mathbf{T}_2^{-1})x - (\mathbf{T}_1^{-1}\boldsymbol{\theta}_{c,1} + \mathbf{T}_2^{-1}\boldsymbol{\theta}_{c,2})\|_\infty}{2} \leq 1 \quad (2.53)$$

The next step is a change of variable to  $\mathbf{v}_3$ . Where  $\mathbf{v}_3$  is constrained to the unit square.

$$\mathbf{v}_3 = \frac{(\mathbf{T}_1^{-1} + \mathbf{T}_2^{-1})\mathbf{x} - (\mathbf{T}_1^{-1}\boldsymbol{\theta}_{c,1} + \mathbf{T}_2^{-1}\boldsymbol{\theta}_{c,2})}{2} \quad (2.54)$$

$$\{\mathbf{x} = 2(\mathbf{T}_1^{-1} + \mathbf{T}_2^{-1})^{-1}\mathbf{v}_3 + (\mathbf{T}_1^{-1} + \mathbf{T}_2^{-1})^{-1}(\mathbf{T}_1^{-1}\boldsymbol{\theta}_{c,1} + \mathbf{T}_2^{-1}\boldsymbol{\theta}_{c,2}), \|\mathbf{v}_3\|_\infty \leq 1\} \quad (2.55)$$

The equation above describes a parallelotope although this form implies three inverse matrix operations. However, if we take into account the identity  $(A^{-1} + B^{-1})^{-1} = A(A + B)^{-1}B = B(A + B)^{-1}A$ , we get,

$$\mathcal{P}_\cap(\mathbf{T}_\cap, \boldsymbol{\theta}_{c,\cap}) = \{\mathbf{x} = 2\mathbf{T}_1(\mathbf{T}_1 + \mathbf{T}_2)^{-1}\mathbf{T}_2\mathbf{v}_3 + \mathbf{T}_2(\mathbf{T}_1 + \mathbf{T}_2)^{-1}\boldsymbol{\theta}_{c,1} + \mathbf{T}_1(\mathbf{T}_1 + \mathbf{T}_2)^{-1}\boldsymbol{\theta}_{c,2}, \|\mathbf{v}_3\|_\infty \leq 1\} \quad (2.56)$$

$$\mathcal{P}_\cap(\mathbf{T}_\cap, \boldsymbol{\theta}_{c,\cap}) = \{\mathbf{x} = \mathbf{T}_\cap\mathbf{v}_3 + \boldsymbol{\theta}_{c,\cap}, \|\mathbf{v}_3\|_\infty \leq 1\} \quad (2.57)$$

### 2.3.3 Vertices of Parallelotopes

The computation of vertices is a well-known problem and is called *vertex enumeration problem*. However, in the case of parallelotopes, this problem has a straightforward solution because there are exactly  $2^n$  vertices and each vertex ( $\mathbf{v}_{p,i}$ ) can be found through,

$$\mathbf{v}_{p,i} = \boldsymbol{\theta}_c + \mathbf{T}\mathbf{v}_i \quad (2.58)$$

where  $\mathbf{v}_{p,i}$  holds  $\|\mathbf{v}_i\|_1 = n$  and  $\|\mathbf{v}_i\|_\infty = 1, \forall i \in [1, 2^n]$ . Clearly, there are  $2^n$  different vectors combinations in  $\mathbb{R}^n$  that hold previous conditions on  $\mathbf{v}_i$ . The matrix  $\mathbf{V}$  is an example of all the possible combinations of  $\mathbf{v}_i$  in  $\mathbb{R}^2$ , this means, that  $\mathbf{V} = [\mathbf{v}_1 \ \mathbf{v}_2 \ \mathbf{v}_3 \ \mathbf{v}_4]$  and is given by

$$\mathbf{V} = \begin{bmatrix} -1 & -1 & 1 & 1 \\ -1 & 1 & -1 & 1 \end{bmatrix} \quad (2.59)$$

if we apply the operations  $\frac{1}{2}(\mathbf{V} + 1)$ , it gets,

$$\frac{1}{2}(\mathbf{V} + 1) = \begin{bmatrix} 0 & 0 & 1 & 1 \\ 0 & 1 & 0 & 1 \end{bmatrix} \equiv [0 \ 1 \ 2 \ 3] \quad (2.60)$$

which is equivalent to the binary numbers between 0 and 3. Thus, one way to compute the vertices of any parallelotope is by using this principle. The Algorithm 1 shows this method.

---

**Algorithm 1** Vertex computation of a parallelotope.

---

**Input:**  $\mathcal{P}(\mathbf{T}, \boldsymbol{\theta}_c)$

1. Get the dimension of  $\mathbf{T}$  and assign it to  $n$ .
2. Build the matrix  $\mathcal{A}_d = [0 \ 1 \ \dots (2^n - 1)]$ .
3. Find the binary representation of each element of  $\mathcal{A}_d$ , This is,  $\mathcal{A}_b := \text{bin}(\mathcal{A}_d)$ .
4. Apply the operation  $\mathcal{A}_b := 2\mathcal{A}_b - 1$
5. **For**  $i = 1$  **to**  $2^n$   
 Compute the matrix  $\mathbf{V}_{p,i} = \boldsymbol{\theta}_c + \mathbf{T}\mathbf{a}_{b,i}$ , where  $\mathbf{a}_{b,i}$  depicts the column  $i$  of  $\mathcal{A}_b$   
**end**

**Output:**  $\mathbf{V}_{p,i}$ .

---

## 2.4 Ellipsoids

### 2.4.1 Definition

Given a vector  $\mathbf{x}_c \in \mathbb{R}^n$ , called the center, and positive definite matrix  $\mathbf{P} \in \mathbb{R}^{n \times n}$ , an ellipsoid is a set that holds the following form,

$$\mathcal{E}(\mathbf{P}, \mathbf{x}_c) = \left\{ \mathbf{x} \in \mathbb{R}^n \mid \sqrt{(\mathbf{x} - \mathbf{x}_c)^\top \mathbf{P} (\mathbf{x} - \mathbf{x}_c)} \leq 1 \right\} \quad (2.61)$$

By defining the root of a positive definite matrix  $\mathbf{P}$  as the unique positive symmetric matrix  $\mathbf{Q} = \mathbf{P}^{-\frac{1}{2}}$  such that  $\mathbf{Q}^2 = \mathbf{P}^{-1}$ , it is possible to derive an alternative dual representation for an ellipsoidal set called generator form:

$$\mathcal{E}(\mathbf{x}_c, \mathbf{Q}) = \{ \mathbf{x} \in \mathbb{R}^n \mid \mathbf{x} = \mathbf{Q}\mathbf{v} + \mathbf{x}_c, \|\mathbf{v}\|_2 \leq 1 \} \quad (2.62)$$

**Proof 4.** *If we go from Equation (2.61) to Equation (2.62),*

$$= \left\{ \mathbf{x} \in \mathbb{R}^n \mid \sqrt{(\mathbf{x} - \mathbf{x}_c)^\top \mathbf{P}^{\frac{1}{2}} \mathbf{P}^{\frac{1}{2}} (\mathbf{x} - \mathbf{x}_c)} \leq 1 \right\} \quad (2.63)$$

$$= \left\{ \mathbf{x} \in \mathbb{R}^n \mid \sqrt{\left( \mathbf{P}^{\frac{1}{2}\top} (\mathbf{x} - \mathbf{x}_c) \right)^\top \mathbf{P}^{\frac{1}{2}} (\mathbf{x} - \mathbf{x}_c)} \leq 1 \right\} \quad (2.64)$$

In this point, we remind that  $\mathbf{P}$  is symmetric, therefore

$$= \left\{ \mathbf{x} \in \mathbb{R}^n \mid \sqrt{\left( \mathbf{P}^{\frac{1}{2}} (\mathbf{x} - \mathbf{x}_c) \right)^\top \mathbf{P}^{\frac{1}{2}} (\mathbf{x} - \mathbf{x}_c)} \leq 1 \right\} \quad (2.65)$$

$$= \left\{ \mathbf{x} \in \mathbb{R}^n \mid \left( \mathbf{P}^{\frac{1}{2}} (\mathbf{x} - \mathbf{x}_c) \right)^\top \mathbf{P}^{\frac{1}{2}} (\mathbf{x} - \mathbf{x}_c) \leq 1 \right\} \quad (2.66)$$

$$= \left\{ \mathbf{x} \in \mathbb{R}^n \mid \left( \mathbf{P}^{\frac{1}{2}} (\mathbf{x} - \mathbf{x}_c) \right)^\top \mathbf{P}^{\frac{1}{2}} (\mathbf{x} - \mathbf{x}_c) \leq 1 \right\} \quad (2.67)$$

If we consider the transformation  $\mathbf{v} = \mathbf{P}^{\frac{1}{2}} (\mathbf{x} - \mathbf{x}_c)$ , we get

$$= \left\{ \mathbf{x} \in \mathbb{R}^n \mid \mathbf{v} = \mathbf{P}^{\frac{1}{2}} (\mathbf{x} - \mathbf{x}_c), \mathbf{v}^\top \mathbf{v} \leq 1 \right\} \quad (2.68)$$

$$= \left\{ \mathbf{x} \in \mathbb{R}^n \mid \mathbf{v} = \mathbf{P}^{\frac{1}{2}} (\mathbf{x} - \mathbf{x}_c), \|\mathbf{v}\|_2 \leq 1 \right\} \quad (2.69)$$

$$= \left\{ \mathbf{x} \in \mathbb{R}^n \mid \mathbf{P}^{-\frac{1}{2}} \mathbf{v} = \mathbf{x} - \mathbf{x}_c, \|\mathbf{v}\|_2 \leq 1 \right\} \quad (2.70)$$

$$= \left\{ \mathbf{x} \in \mathbb{R}^n \mid \mathbf{x} = \mathbf{x}_c + \mathbf{P}^{-\frac{1}{2}} \mathbf{v}, \|\mathbf{v}\|_2 \leq 1 \right\} \quad (2.71)$$

Finally, it is assumed  $\mathbf{Q} = \mathbf{P}^{-\frac{1}{2}}$  and is got equation (2.62).

## 2.4.2 Basic Operation with Ellipsoids

### 2.4.2.1 Linear Transformation

Given ellipsoids  $\mathcal{E}_1(\mathbf{Q}_1, \mathbf{x}_{c,1})$  and  $\mathcal{E}_2(\mathbf{Q}_2, \mathbf{x}_{c,2})$ . It is said that  $\mathcal{E}_2(\mathbf{Q}_2, \mathbf{x}_{c,2})$  is linear transformation of  $\mathcal{E}_1(\mathbf{Q}_1, \mathbf{x}_{c,1})$  if and only if, exists a nonsingular matrix  $\mathbf{S} \in \mathbb{R}^{n \times n}$  and a linear relation  $\mathbf{x}_2 = \mathbf{S}\mathbf{x}_1 + \mathbf{q}$  with  $\mathbf{q} \in \mathbb{R}^{n \times 1}$ . Therefore,

$$\mathbf{Q}_2 = \mathbf{S}\mathbf{Q}_1 \quad \mathbf{x}_{c,2} = \mathbf{S}\mathbf{x}_{c,1} + \mathbf{q} \quad (2.72)$$

The demonstration of this property is similar to the linear transformation of parallelo-tope (See 2.3.2.1).

### 2.4.2.2 Minkowski Sum

Ellipsoid are not closed under Minkowski sum. [18] proposed an outer approximation of the Minkowski sum of  $k$  ellipsoids that is given by,

$$\mathbf{x}_c = \sum_{i=1}^k \mathbf{x}_{c,i} \quad \mathbf{Q}(\mathbf{r}) = \left( \sum_{i=1}^k \sqrt{\mathbf{r}^\top \mathbf{Q}_i \mathbf{r}} \right) \sum_{i=1}^k \frac{\mathbf{Q}_i}{\sqrt{\mathbf{r}^\top \mathbf{Q}_i \mathbf{r}}} \quad \forall \mathbf{r}^\top \mathbf{r} = 1 \quad (2.73)$$

A complete demonstration is found in [18].

## 2.5 Zonotopes

### 2.5.1 Definition

Zonotopes are a special class of symmetric convex sets. They can be described in terms of polyhedron or polytopes. Therefore, the properties of polytopes and polyhedron apply to zonotopes. The zonotopes can be defined as the Minkowski sum of  $m$  line segments in  $\mathbb{R}^n$ . This is the way used by [12], and it is expressed as,

$$\mathcal{Z}(\mathbf{T}, \boldsymbol{\theta}_c) = \{\mathbf{x} = \mathbf{T}\mathbf{v} + \boldsymbol{\theta}_c, \|\mathbf{v}\|_\infty \leq \mathbf{1}\} \quad (2.74)$$

where  $\mathbf{T} \in \mathbb{R}^{m \times n}$ , and it is called the generator form. In the same way than parallelotopes, the columns of  $\mathbf{T}$  are called generators.

### 2.5.2 Basic Operations with Zonotopes

#### 2.5.2.1 Linear Transformation

Given zonotopes  $\mathcal{Z}_1(\mathbf{T}_1, \boldsymbol{\theta}_{c,1})$  and  $\mathcal{Z}_2(\mathbf{T}_2, \boldsymbol{\theta}_{c,2})$ . It is said that  $\mathcal{Z}_2(\mathbf{T}_2, \boldsymbol{\theta}_{c,2})$  is linear transformation of  $\mathcal{Z}_1(\mathbf{T}_1, \boldsymbol{\theta}_{c,1})$  if and only if, exists a nonsingular matrix  $\mathbf{S} \in \mathbb{R}^{n \times n}$  and a linear relation  $\mathbf{x}_2 = \mathbf{S}\mathbf{x}_1 + \mathbf{L}$  with  $\mathbf{q} \in \mathbb{R}^{n \times 1}$ . Therefore,

$$\mathbf{T}_2 = \mathbf{S}\mathbf{T}_1 \quad \boldsymbol{\theta}_{c,2} = \mathbf{S}\boldsymbol{\theta}_{c,1} + \mathbf{q} \quad (2.75)$$

The demonstration of this property is similar to the linear transformation of parallelotope and ellipsoids (See 2.3.2.1).

#### 2.5.2.2 Minkowski Sum

Zonotopes are closed under Minkowski sum. This operation is determined in the following way. Given zonotopes  $\mathcal{Z}_1(\mathbf{T}_1, \boldsymbol{\theta}_{c,1})$  and  $\mathcal{Z}_2(\mathbf{T}_2, \boldsymbol{\theta}_{c,2})$ . The Minkowski sum is given by,

$$\mathbf{T}_s = [\mathbf{T}_1 \quad \mathbf{T}_2] \quad \boldsymbol{\theta}_{c,s} = \boldsymbol{\theta}_{c,1} + \boldsymbol{\theta}_{c,2} \quad (2.76)$$

**Proof 5.** The Minkowski sum is defined as  $\mathbf{x}_3 = \mathbf{x}_1 + \mathbf{x}_2$ . Thus,

$$\mathbf{x}_3 = \mathbf{x}_1 + \mathbf{x}_2 \quad (2.77)$$

$$\mathbf{x}_3 = \mathbf{T}_1 \mathbf{v}_1 + \boldsymbol{\theta}_{c,1} + \mathbf{T}_2 \mathbf{v}_2 + \boldsymbol{\theta}_{c,2}, \|\mathbf{v}_1\|_\infty \leq 1, \|\mathbf{v}_2\|_\infty \leq 1 \quad (2.78)$$

$$\mathbf{x}_3 = [\mathbf{T}_1 \ \mathbf{T}_2] \begin{bmatrix} \mathbf{v}_1 \\ \mathbf{v}_2 \end{bmatrix} + \boldsymbol{\theta}_{c,1} + \boldsymbol{\theta}_{c,2}, \left\| \begin{bmatrix} \mathbf{v}_1 \\ \mathbf{v}_2 \end{bmatrix} \right\|_\infty \leq 1 \quad (2.79)$$

Clearly, the equation (2.79) depicts a zonotope.

## 2.6 Polytopes

### 2.6.1 Definition

A polytope is a set of inequalities (half-spaces) with a compact and bounded solution. It is a bounded polyhedron or the finite intersection of  $m$  half-spaces. Polytopes can be depicted by showing the whole set of inequalities. This way, it is recognized such as half-space representation or just  $\mathcal{H}$ -Rep or towards its convex hull, in which case is known as vertex representation or just  $\mathcal{V}$ -Rep. Each representation has advantages and drawbacks against each other for different operations. For example, Minkowski sum is easily computed in  $\mathcal{V}$ -Rep, but it is not an easy task for linear transformations, while it is the contrary for  $\mathcal{H}$ -Rep polytope.

### 2.6.2 Half-Space Representation

An arbitrary polytope  $P$  is given in  $\mathcal{H}$ -Rep if it is represented as,

$$P = \{\mathbf{x} | \mathbf{G}\mathbf{x} \leq \mathbf{h}\} \quad (2.80)$$

where  $\mathbf{G} \in \mathbb{R}^{m \times n}$  and it is called facet matrix and  $\mathbf{h} \in \mathbb{R}^{m \times 1}$  is known as offset or constant vector.

### 2.6.3 Vertex Representation

An arbitrary polytope  $P$  is given in  $\mathcal{V}$ -Rep if it is represented as,

$$P = \left\{ \sum_{i=1}^p \alpha_i v_i, \forall \alpha_i \geq 0, \sum_{i=1}^p \alpha_i = 1 \right\} \quad (2.81)$$

where  $v_i \in \mathbb{R}^{n \times 1}$  and are the vertices and  $\alpha_i \in \mathbb{R}$ .

### 2.6.4 Basic Operations with Polytopes in $\mathcal{H}$ -Rep

This section reviews computational methods from the field of polytopic set arithmetic. The polytopes are closed under intersection, linear transformations as well as under Minkowski sums (see Blanchini and Miani [8]). As many of these operations increase the complexity of the resulting polytopes, one needs to implement facet reduction operations in order to not run out of memory and to keep the computational time within reasonable bounds. The following propositions summarize practical procedures for implementing such facet-reduction steps.

#### 2.6.4.1 Intersection

The intersection of two polytopes is an operation where their elements belong to both involved polytopes. Let  $P_1(\mathbf{G}_1, \mathbf{h}_1)$  and  $P_2(\mathbf{G}_2, \mathbf{h}_2)$  be given polytopes. Then,

$$P_1(\mathbf{G}_1, \mathbf{h}_1) \cap P_2(\mathbf{G}_2, \mathbf{h}_2) \equiv P_\cap([\mathbf{G}_1^\top \quad \mathbf{G}_2^\top]^\top, [\mathbf{h}_1^\top \quad \mathbf{h}_2^\top]^\top) \quad (2.82)$$

**Proof 6.** *Only those elements that belongs to  $P_1$  and  $P_2$  are in the intersection. This statement can be expressed as,*

$$P_\cap = \mathbf{G}_1 \mathbf{x} \leq \mathbf{h}_1, \quad \mathbf{G}_2 \mathbf{x} \leq \mathbf{h}_2 \quad (2.83)$$

Now, because both conditions depend on the same variable, we can enclose them as,

$$P_\cap = \begin{bmatrix} \mathbf{G}_1 \\ \mathbf{G}_2 \end{bmatrix} \mathbf{x} \leq \begin{bmatrix} \mathbf{h}_1 \\ \mathbf{h}_2 \end{bmatrix} \quad (2.84)$$

#### 2.6.4.2 Scaling or Linear Transformation

Let  $P_1(\mathbf{G}_1, \mathbf{h}_1)$  and  $P_2(\mathbf{G}_2, \mathbf{h}_2)$  be given polytopes and a linear relation between both sets of the form  $\mathbf{x}_2 = \mathbf{S}\mathbf{x}_1 + \mathbf{a}$  with  $\mathbf{S}$  being a nonsingular matrix. Then, it is said that  $P_2$  is a linear transformation of  $P_1$  and it is given by

$$P_2(\mathbf{G}_2, \mathbf{h}_2) = P_1(\mathbf{G}_1 \mathbf{S}^{-1}, \mathbf{h}_1 + \mathbf{G}_1 \mathbf{S}^{-1} \mathbf{a}) \quad (2.85)$$

In case, vector  $\mathbf{a}$  is a null vector. Then, it is said that  $P_1$  have been **scaled or mapped**.

**Proof 7.** *First, it is found  $\mathbf{x}_1$ ,*

$$\mathbf{x}_2 = \mathbf{S}\mathbf{x}_1 + \mathbf{a} \quad (2.86)$$

$$\mathbf{x}_1 = \mathbf{S}^{-1}(\mathbf{x}_2 - \mathbf{a}) \quad (2.87)$$

$$\mathbf{x}_1 = \mathbf{S}^{-1}\mathbf{x}_2 - \mathbf{S}^{-1}\mathbf{a} \quad (2.88)$$

Using the polytope definition, we get

$$P_1 = \{\mathbf{x}_1 | \mathbf{G}_1 \mathbf{x}_1 \leq \mathbf{h}_1\} \quad (2.89)$$

$$\Rightarrow \{\mathbf{x}_2 | \mathbf{G}_1 (\mathbf{S}^{-1} \mathbf{x}_2 - \mathbf{S}^{-1} \mathbf{a}) \leq \mathbf{h}_1\} \quad (2.90)$$

$$P_2 = \{\mathbf{x}_2 | \mathbf{G}_1 \mathbf{S}^{-1} \mathbf{x}_2 - \mathbf{G}_1 \mathbf{S}^{-1} \mathbf{a} \leq \mathbf{h}_1\} \quad (2.91)$$

$$P_2 = \{\mathbf{x}_2 | \mathbf{G}_1 \mathbf{S}^{-1} \mathbf{x}_2 \leq \mathbf{h}_1 + \mathbf{G}_1 \mathbf{S}^{-1} \mathbf{a}\} \quad (2.92)$$

### 2.6.4.3 Facet Reduction

Let  $P_1(\mathbf{G}_1, \mathbf{h}_1)$  be a given polytope. Then

$$P_1(\mathbf{G}_1, \mathbf{h}_1) \subseteq P(\mathbf{\Lambda}^\top \mathbf{G}_1, \mathbf{\Lambda}^\top \mathbf{h}_1)$$

for any  $\mathbf{\Lambda} \geq 0$  (componentwise),  $\mathbf{\Lambda} \in \mathbb{R}^{m \times w}$ . without loss of generality, we may assume  $\|\mathbf{\Lambda}\| = 1$ .

**Proof 8.** First, we assume that the resulting facet matrix after the reduction is given

and is  $\mathbf{G} = \begin{bmatrix} \mathbf{g}_1^\top \\ \mathbf{g}_2^\top \\ \vdots \\ \mathbf{g}_w^\top \end{bmatrix}$ . Thus, the constant vector is obtained by the following maximization.

$$\max_{\mathbf{x}_1} \mathbf{g}_i^\top \mathbf{x}_1 \quad (2.93)$$

$$\text{s.t. } \mathbf{G}_1 \mathbf{x}_1 \leq \mathbf{h}_1$$

The Lagrangian ( $L$ ) with multiplier  $\lambda_i \in \mathbb{R}^{m \times 1}$  of this problem is given by,,

$$L(\mathbf{x}_1, \lambda_i) = \mathbf{g}_i^\top \mathbf{x}_1 + \lambda_i^\top (\mathbf{G}_1 \mathbf{x}_1 - \mathbf{h}_1) \quad (2.94)$$

After ordering in a proper way,

$$L(\mathbf{x}_1, \lambda_i) = \lambda_i^\top \mathbf{G}_1 \mathbf{x}_1 + \mathbf{g}_i^\top \mathbf{x}_1 - \lambda_i^\top \mathbf{h}_1 \quad (2.95)$$

Now, if we only focus on the maximization of the first two elements. We notice that the conjugate function definition can apply (See section 2.1.2 and the proof 9). Therefore,

$$\max_{\lambda_i} -\lambda_i^\top \mathbf{h}_1 \quad (2.96)$$

$$\text{s.t. } \lambda_i^\top \mathbf{G}_1 = \mathbf{g}_i^\top$$

$$\lambda_i \geq 0$$

Now, it is possible to write dual optimization problem

$$\begin{aligned} \min_{\lambda_i} \lambda_i^\top \mathbf{h}_1 & \quad (2.97) \\ \text{s.t. } \lambda_i^\top \mathbf{G}_1 &= \mathbf{g}_i^\top \\ \lambda_i &\geq 0 \end{aligned}$$

Finally, the solution of the equation above results in the value of  $h_i$ . It is clear that for each  $\mathbf{g}_i$  there will exist a multiplier that minimize the objective. Therefore, the intersection of all these multipliers will bring up our condition as,

$$\mathbf{\Lambda} = [\lambda_1 \quad \lambda_2 \quad \cdots \quad \lambda_w] \quad (2.98)$$

**Remark 2.** It is important to notice that these are necessary but do not sufficient conditions to compute facet reduction because we do not know with certainty the resulting reduced facet matrix. However, it is still possible to compute the facet using good guess for  $\mathbf{G}$ .

#### 2.6.4.4 Minkowski Sum

The Minkowski sum is a computationally expensive operation that requires either vertex enumeration and convex hull computation in  $\mathbb{R}^n$  or a projection from  $\mathbb{R}^{2n}$  down to  $\mathbb{R}^n$ , Baotic [5].

However, in this work, we propose another approach.

Let  $P_1(\mathbf{G}_1, \mathbf{h}_1)$  and  $P_2(\mathbf{G}_2, \mathbf{h}_2)$  be given polytopes, with facets matrices  $\mathbf{G}_1 \in \mathbb{R}^{m \times n}$  and  $\mathbf{G}_2 \in \mathbb{R}^{p \times n}$ . Then

$$P_1(\mathbf{G}_1, \mathbf{h}_1) \oplus P_2(\mathbf{G}_2, \mathbf{h}_2) \subseteq P(\mathbf{\Lambda}_1^\top \mathbf{G}_1, \mathbf{\Lambda}_1^\top \mathbf{h}_1 + \mathbf{\Lambda}_2^\top \mathbf{h}_2) \quad (2.99)$$

for any  $\mathbf{\Lambda}_1, \mathbf{\Lambda}_2 \geq 0$  with  $\mathbf{\Lambda}_1^\top \mathbf{G}_1 = \mathbf{\Lambda}_2^\top \mathbf{G}_2$ .

**Proof 9.** To demonstrate this property, we assume that the resulting facet matrix

is known, and is  $\mathbf{G} = \begin{bmatrix} \mathbf{g}_1^\top \\ \mathbf{g}_2^\top \\ \vdots \\ \mathbf{g}_i^\top \end{bmatrix}$ . Thus, the constant vector is obtained by the support

function of the resulting polytope throughout all  $\mathbf{g}_i$ . The support function around  $\mathbf{g}_i$  is given by,

$$\sigma[\mathbf{P}](\mathbf{g}_i) = \sigma[\mathbf{P}_1](\mathbf{g}_i) + \sigma[\mathbf{P}_2](\mathbf{g}_i) \quad (2.100)$$

$$= \max_{\mathbf{x}_1} \mathbf{g}_i^\top \mathbf{x}_1 \quad + \quad \max_{\mathbf{x}_2} \mathbf{g}_i^\top \mathbf{x}_2 \quad (2.101)$$

$$\text{s.t. } \mathbf{G}_1 \mathbf{x}_1 \leq \mathbf{h}_1 \quad \text{s.t. } \mathbf{G}_2 \mathbf{x}_2 \leq \mathbf{h}_2$$

We can reduce these problems to only one in the following way,

$$\max_{\mathbf{x}_1, \mathbf{x}_2} [\mathbf{g}_i^\top \quad \mathbf{g}_i^\top] \begin{bmatrix} \mathbf{x}_1 \\ \mathbf{x}_2 \end{bmatrix} \quad (2.102)$$

$$\text{s.t. } \mathbf{G}_1 \mathbf{x}_1 \leq \mathbf{h}_1$$

$$\mathbf{G}_2 \mathbf{x}_2 \leq \mathbf{h}_2$$

The Lagrangian ( $L$ ) with multipliers  $\lambda_{i,1} \in \mathbb{R}^{m \times 1}$  and  $\lambda_{i,2} \in \mathbb{R}^{p \times 1}$  of this problem is given by,

$$L(\mathbf{x}_1, \mathbf{x}_2, \lambda_{i,1}, \lambda_{i,2}) = [\mathbf{g}_i^\top \quad \mathbf{g}_i^\top] \begin{bmatrix} \mathbf{x}_1 \\ \mathbf{x}_2 \end{bmatrix} + \lambda_{i,1}^\top (\mathbf{G}_1 \mathbf{x}_1 - \mathbf{h}_1) + \lambda_{i,2}^\top (\mathbf{G}_2 \mathbf{x}_2 - \mathbf{h}_2) \quad (2.103)$$

After ordering in a proper way,

$$L(\mathbf{x}_1, \mathbf{x}_2, \lambda) = \lambda_{i,1}^\top \mathbf{G}_1 \mathbf{x}_1 + \lambda_{i,2}^\top \mathbf{G}_2 \mathbf{x}_2 + [\mathbf{g}_i^\top \quad \mathbf{g}_i^\top] \begin{bmatrix} \mathbf{x}_1 \\ \mathbf{x}_2 \end{bmatrix} - \lambda_{i,1}^\top \mathbf{h}_1 - \lambda_{i,2}^\top \mathbf{h}_2 \quad (2.104)$$

$$= \underbrace{\left[ \lambda_{i,1}^\top \mathbf{G}_1 \quad \lambda_{i,2}^\top \mathbf{G}_2 \right]}_{\text{underbrace part}} \begin{bmatrix} \mathbf{x}_1 \\ \mathbf{x}_2 \end{bmatrix} + [\mathbf{g}_i^\top \quad \mathbf{g}_i^\top] \begin{bmatrix} \mathbf{x}_1 \\ \mathbf{x}_2 \end{bmatrix} - \lambda_{i,1}^\top \mathbf{h}_1 - \lambda_{i,2}^\top \mathbf{h}_2 \quad (2.105)$$

Now, if we only focus on the maximization of the underbrace part. We notice that the conjugate function definition can apply (See section 2.1.2). Therefore,

$$\max_{\lambda_{i,1}, \lambda_{i,2}} -\lambda_{i,1}^\top \mathbf{h}_1 - \lambda_{i,2}^\top \mathbf{h}_2 \quad (2.106)$$

$$\text{s.t. } \lambda_{i,1}^\top \mathbf{G}_1 = \lambda_{i,2}^\top \mathbf{G}_2$$

$$\lambda_{i,1} \geq 0, \lambda_{i,2} \geq 0$$

On this configuration, it is possible to write dual optimization problem

$$\min_{\lambda_{i,1}, \lambda_{i,2}} \lambda_{i,1}^\top \mathbf{h}_1 + \lambda_{i,2}^\top \mathbf{h}_2 \quad (2.107)$$

$$\text{s.t. } \lambda_{i,1}^\top \mathbf{G}_1 = \lambda_{i,2}^\top \mathbf{G}_2$$

$$\lambda_{i,1} \geq 0, \lambda_{i,2} \geq 0$$

Finally, the solution of the equation above results in the value of  $h_i$ . It is clear that for each  $\mathbf{g}_i$  there will exist a pair of multipliers. Therefore, the intersection of all these multipliers will bring up our condition as,

$$\Lambda_1 = [\lambda_{1,1} \quad \lambda_{2,1} \quad \cdots \quad \lambda_{i,1}] \quad \Lambda_2 = [\lambda_{1,2} \quad \lambda_{2,2} \quad \cdots \quad \lambda_{i,2}] \quad (2.108)$$

**Remark 3.** It is important to notice that these are necessary but do not sufficient conditions to compute the Minkowski sum because we do not know with certainty the resulting facet matrix. However, it is still possible to compute the Minkowski sum using good guess for  $\mathbf{G}$ .

## 2.6.5 Geometric Problems with Polytopes

### 2.6.5.1 Redundancy Removal

Let  $P$  be a polytope build up by  $m$  half-spaces,  $\mathcal{H}_i(\mathbf{g}_i, h_i) = \{\mathbf{x}_i \in \mathbb{R}^n \mid \mathbf{g}_i^\top \mathbf{x}_i \leq h_i\} \forall i \in \{1, 2, 3, \dots, m\}$ . Then, it is said that  $\mathcal{H}_i$  is redundant, if and only if, after we remove  $\mathcal{H}_i$ , the polytope holds invariant. One way to solve this problem is by testing all  $\mathcal{H}_i$  such as,

$$\begin{aligned} \max_{\mathbf{x}} \mathbf{g}_i^\top \mathbf{x} & & (2.109) \\ \text{s.t. } \mathbf{G}_{i-} \mathbf{x} &\leq \mathbf{h}_{i-} \\ \mathbf{g}_i^\top \mathbf{x} &\leq h_i + a \end{aligned}$$

where  $\mathbf{G}_{i-} = [\mathbf{g}_1, \dots, \mathbf{g}_{i-1}, \mathbf{g}_{i+1}, \dots, \mathbf{g}_m]^\top$ , in the same way,  $\mathbf{h}_{i-} = [h_1, \dots, h_{i-1}, h_{i+1}, \dots, h_m]^\top$  and  $a$  is any positive constant, usually 1. A simple algorithm to solve this problem is shown in Baotic [5].

### 2.6.5.2 Centering

The most common approach to establish a quasi center of a polytope is to use is the Chebyshev ball. Figure 2.7 shows an example of the use of Chebyshev center. This is the biggest ball inside of a polytope. The center  $\mathbf{x}_c$  of this ball is the deepest point inside  $P$  in the sense that it is farthest from the exterior. If the polytope is not empty,

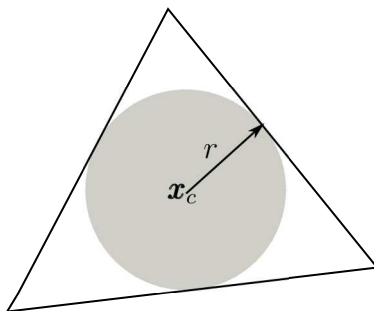


**Figure 2.7:** Example of a Chebyshev ball in a polytope of two dimensions.

then, the Chebyshev center can be computed as,

$$\begin{aligned} \max_r \quad & r \\ \text{s.t.} \quad & \mathbf{g}_i^\top \mathbf{x} + r \|\mathbf{g}_i\|_2 \leq h_i \end{aligned} \tag{2.110}$$

# Set-Membership State Estimation and Control

---

Once the theoretical foundation has been established, Set-membership State Estimation (SSE) is brought up. This chapter introduces the principles of SSE around any convex set. Furthermore in the particular case of parallelotopes and polytopes some algorithms and examples are shown. In addition, a robust MPC is designed using the results of the estimation.

## 3.1 The System in Consideration

Given a discrete nonlinear invariant dynamic system with bounded mismatches in the processes (uncertainties) and bounded errors in the measurement output of the form,

$$\mathbf{x}_{k+1} = \mathbf{f}(\mathbf{x}_k, \mathbf{u}_k, \boldsymbol{\omega}_k) \quad (3.1)$$

$$\mathbf{y}_{m,k} = \mathbf{h}(\mathbf{x}_k, \boldsymbol{\nu}_k) \quad (3.2)$$

where  $k \in \mathbb{N}$  means step time,  $\mathbf{x}_k \in \mathbb{R}^n$  denotes the state vector of the system and  $\mathbf{y}_{m,k} \in \mathbb{R}^{n_o}$  the measurement output,  $\mathbf{u}_k \in \mathbb{R}^{n_u}$  the control input, and  $\boldsymbol{\omega}_k \in \Omega \subset \mathbb{R}^{n_\omega}$  and  $\boldsymbol{\nu}_k \in \Psi \subset \mathbb{R}^{n_\nu}$  are the uncertainties and disturbances measurements, respectively. Assuming that  $f$  and  $h$  are continuous and differentiable on  $\mathbf{x}$ ,  $\mathbf{u}$ ,  $\boldsymbol{\omega}$ , and  $\boldsymbol{\nu}$ , it is possible to split the equations into linear and nonlinear parts around one particular initial conditions  $(\mathbf{x}_0, \mathbf{u}_0, \boldsymbol{\omega}_0, \boldsymbol{\nu}_0)$ . This is,

$$\mathbf{x}_{k+1} = \mathbf{A}\mathbf{x}_k + \mathbf{B}\mathbf{u}_k + \mathbf{E}\boldsymbol{\omega}_k + \boldsymbol{\gamma}_f(\mathbf{x}_k, \mathbf{u}_k, \boldsymbol{\omega}_k) \quad (3.3)$$

$$\mathbf{y}_{m,k} = \mathbf{C}\mathbf{x}_k + \mathbf{F}\boldsymbol{\nu}_k + \boldsymbol{\eta}_h(\mathbf{x}_k, \boldsymbol{\nu}_k) \quad (3.4)$$

where  $\mathbf{A} \in \mathbb{R}^{n \times n}$  is the state matrix,  $\mathbf{B} \in \mathbb{R}^{n \times n_u}$  the input matrix,  $\mathbf{E} \in \mathbb{R}^{n \times n_\omega}$  the uncertain matrix. These matrices are found by the Jacobian of  $f$  with each variable, this is,

$$\mathbf{A} = \left. \frac{\partial \mathbf{f}}{\partial \mathbf{x}} \right|_{\mathbf{x}_0, \mathbf{u}_0, \boldsymbol{\omega}_0} \quad \mathbf{B} = \left. \frac{\partial \mathbf{f}}{\partial \mathbf{u}} \right|_{\mathbf{x}_0, \mathbf{u}_0, \boldsymbol{\omega}_0} \quad \mathbf{E} = \left. \frac{\partial \mathbf{f}}{\partial \boldsymbol{\omega}} \right|_{\mathbf{x}_0, \mathbf{u}_0, \boldsymbol{\omega}_0} \quad (3.5)$$

in the same way, matrices  $\mathbf{C} \in \mathbb{R}^{n_o \times n}$  the output matrix,  $\mathbf{F} \in \mathbb{R}^{n_o \times n_\nu}$  the noise matrix can be found by,

$$\mathbf{C} = \left. \frac{\partial \mathbf{h}}{\partial \mathbf{x}} \right|_{x_0, \nu_0} \quad \mathbf{F} = \left. \frac{\partial \mathbf{h}}{\partial \nu} \right|_{x_0, \nu_0} \quad (3.6)$$

Finally  $\gamma_f$  and  $\eta_h$  depict nonlinearities in the model. The output of the system can be always substituted by a linear output through the addition of an auxiliary state. The auxiliary state can take the form,

$$\mathbf{x}_{a,k} = \mathbf{C}\mathbf{x}_k + \eta_h(\mathbf{x}_k, \nu_k) \quad (3.7)$$

where its difference equation is deduced by,

$$\mathbf{x}_{a,k+1} = \mathbf{C}\mathbf{x}_{k+1} + \eta_{h,k+1} \quad (3.8)$$

$$\mathbf{x}_{a,k+1} = \mathbf{C}(\mathbf{A}\mathbf{x}_k + \mathbf{B}\mathbf{u}_k + \mathbf{E}\omega_k + \gamma_{f,k}) + \eta_{h,k+1} \quad (3.9)$$

$$\mathbf{x}_{a,k+1} = \mathbf{C}\mathbf{A}\mathbf{x}_k + \mathbf{C}\mathbf{B}\mathbf{u}_k + \mathbf{C}\mathbf{E}\omega_k + \mathbf{C}\gamma_{f,k} + \eta_{h,k+1} \quad (3.10)$$

If we add the new auxiliary state of the Equation (3.10) into the state equation found in (3.3), then, it is possible to re-formulate a new linear system of  $n + n_o$  states. On the following way,

$$\mathbf{z}_{k+1} = \widehat{\mathbf{A}}\mathbf{z}_k + \widehat{\mathbf{B}}\mathbf{u}_k + \widehat{\mathbf{E}}\omega_k + \widehat{\gamma}_f(\mathbf{z}_k, \mathbf{u}_k, \omega_k) \quad (3.11)$$

$$\mathbf{y}_{m,k} = \widehat{\mathbf{C}}\mathbf{z}_k + \mathbf{F}\nu_k \quad (3.12)$$

where,

$$\widehat{\mathbf{A}} = \begin{bmatrix} \mathbf{A} & \mathbf{0}_n \\ \mathbf{C}\mathbf{A} & \mathbf{0}_{n_o} \end{bmatrix} \quad \widehat{\mathbf{B}} = \begin{bmatrix} \mathbf{B} \\ \mathbf{C}\mathbf{B} \end{bmatrix} \quad \widehat{\mathbf{E}} = \begin{bmatrix} \mathbf{E} \\ \mathbf{C}\mathbf{E} \end{bmatrix} \quad \widehat{\mathbf{C}} = [\mathbf{0}_{n_o \times n} \quad I_{n_o}] \quad (3.13)$$

$$\widehat{\gamma}_f = \begin{bmatrix} \gamma_f \\ \mathbf{C}\gamma_f + \eta_{h,k+1} \end{bmatrix} \quad (3.14)$$

At this point, we already have the representation of the system we are focus on. However, for keeping the standard notation, we are going to change variable  $\mathbf{z}$  by  $\mathbf{x}$  and the constants  $\widehat{\mathbf{A}}, \widehat{\mathbf{B}}, \widehat{\mathbf{E}}, \widehat{\mathbf{C}}$  for the usual letters. This is,

$$\mathbf{x}_{k+1} = \mathbf{A}\mathbf{x}_k + \mathbf{B}\mathbf{u}_k + \mathbf{E}\omega_k + \gamma_f(\mathbf{x}_k, \mathbf{u}_k, \omega_k) \quad (3.15)$$

$$\mathbf{y}_{m,k} = \mathbf{C}\mathbf{x}_k + \mathbf{F}\nu_k \quad (3.16)$$

**Remark 4.** *It is important to mention that in this work, we do not distinguish explicitly between states and parameters. Here, we recall that parameters can be regarded as constant states, which satisfy the trivial recursion  $\mathbf{p}_{k+1} = \mathbf{p}_k$ . In this sense, it is sufficient to analyze nonlinear systems of the form (3.1), although the structure of the function  $f$  needs to be exploited by numerical methods if trivial constant recursions for parameters are stacked.*

## 3.2 Set-membership State Estimation

The set-membership state estimation problem consists of finding the smallest set that contains the unknown state and/or unknown parameters updating constantly with the measurement output of the system. This is also called "guaranteed estimation" because of the estimation process always computes a region with the true value of the system. Available methods based on SSE approaches exist for linear and non-linear models (see 1 for more details). In this context, all authors consider the following assumptions.

**Assumption 1.** *The set is known where the true value of the system state lies.*

**Assumption 2.** *The uncertainties and noises in the system are unknown, however, their maximum absolute values are bounded and known.*

**Assumption 3.** *There is an accurate system model for the linear dynamics and known boundaries for the nonlinear behaviour. It means that matrices in (3.15) and (3.16) are known.*

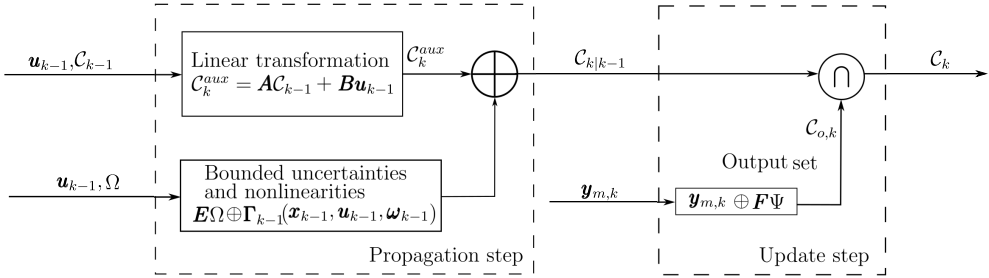


**Figure 3.1:** General diagram of a set-membership state estimation approach

SSE is based on the construction of a compact set that includes, with guarantee, the states of the system that are consistent with the measured output and take into account the bounded noise. One of the main goals is to compute bounds on the set of trajectories systems that are consistent with the measured outputs. Overall, SSE splits into two steps. The propagation, where the chosen set must be "moved" accordingly to the dynamics of the plant and increases its size based on the uncertainty bounded of the process and the update step, where the chosen set must be intersected with the measurement output set,  $\mathcal{C}_{o,k}$ . A complete diagram of SSE is shown in the Figure 3.1. In this figure, there are two dashed line boxes where the intersection and update step are included. In a general view, the required inputs, outputs and also operations to perform each step are shown. Next sections will describe in detail these steps.

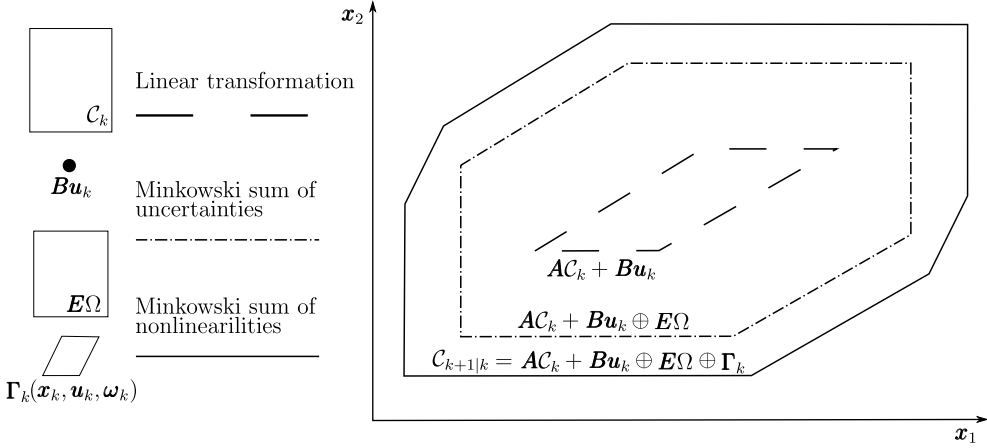


Figure 3.2: The propagation step.

### 3.2.1 Propagation

The propagation step concerns the application of convex set operations over a known set (see Assumption 1) in order to ensure that the resulting set contains the system state vector of the next step time. To perform this task, the convex set ( $\mathcal{C}_k$ ) has to follow the behavior of the dynamic system, Equation (3.15).

In general, SSE is developed through a recursive algorithm, hence,  $\mathcal{C}_k$  is the resulting set from the previous step time. Therefore, after this step, the resulting set is known as the predictive set or simply propagated set and in this work is depicted as  $\mathcal{C}_{k+1|k}$  to represent an intermediate step.

The propagation process can be expressed in the following way. Given a fixed convex set  $\mathcal{C}_k$ , where it is known that  $\mathbf{x}_k \in \mathcal{C}_k$ . The propagation process is given by,

$$\mathcal{C}_{k+1|k} = \mathbf{A}\mathcal{C}_k \oplus \mathbf{B}\mathbf{u}_k \oplus \mathbf{E}\Omega \oplus \Gamma_k(\mathbf{x}_k, \mathbf{u}_k, \boldsymbol{\omega}_k) \quad (3.17)$$

where  $\mathcal{C}_{k+1|k}$  (the prediction set) depicts the convex set that guarantees to enclose  $\mathbf{x}_{k+1}$  and  $\Gamma_k$  is a convex set built with the bound of the nonlinear function  $\gamma_f(\mathbf{x}_k, \mathbf{u}_k, \boldsymbol{\omega}_k)$ . To compute Equation (3.17), it is necessary to perform the linear transformations of all sets involved, and after computing the Minkowski sum. A graphic representation of this step is shown in the Figure 3.2. The figure shows how the convex set turns into a new one for guaranteeing the state system of the iteration  $k + 1$ .

**Remark 5.** Details on how to construct nonlinearity bounds  $\Gamma_k$  can be found in [32]

*in a slightly different context, but the corresponding methods can be applied for state estimation problems, too.*

### 3.2.2 Update

The update step or intersection step concerns computing the exact (or an over-approximation of) intersection between the propagated set and the output set. The output set is built with the measurement output and the noises bounds. A

$$\mathcal{C}_{o,k} = \{\mathbf{x}_k \in \mathbb{R}^n \mid \mathbf{C}\mathbf{x}_k - \mathbf{y}_{m,k} \in \mathbf{F}\Psi\} \quad (3.18)$$

and it denotes the set of states that are consistent with the measurement outputs. In the same way, this set can be represented as a combination of  $n_o$  sets, one for each output or just one set. This lead to two different ways to compute SSE called sequential and block approaches.

The intersection step is formulated to find the intersection between  $\mathcal{C}_{o,k}$  and  $\mathcal{C}_{k|k-1}$  and it can be expressed as,

$$\mathcal{C}_k = \mathcal{C}_{k|k-1} \cap \mathcal{C}_{o,k} \quad (3.19)$$

Notice that an exact computation of the set 3.19 is in general nontractable, because of sets increase their complexity after each step time that brings high computational cost. Therefore, this equation is usually reformulated as,

$$\mathcal{C}_{k|k-1} \cap \mathcal{C}_{o,k} \subset \mathcal{C}_k \quad (3.20)$$

The Figure 3.3 shows a simple example of this step. In this case, the intersection (gray area) can be enclosed using the interval hull of the operation (dot line) or the minimum paralleloptope(dash line).

The computation of the output set can be found through two different methods when multiple outputs are considered. These methods are presented below together their advantages and disadvantages. These approaches produce the same result when the exact intersection is found although the computational cost will vary. But for high dimensional cases, the exact intersection is not tractable, hence, we always assume an overapproximation of this set.

#### 3.2.2.1 Sequential Approach

This approach focuses on building  $n_o$  output sets, one for each output. It follows by the computation of  $n_o$  intersections (actually, over-approximations of the intersection)

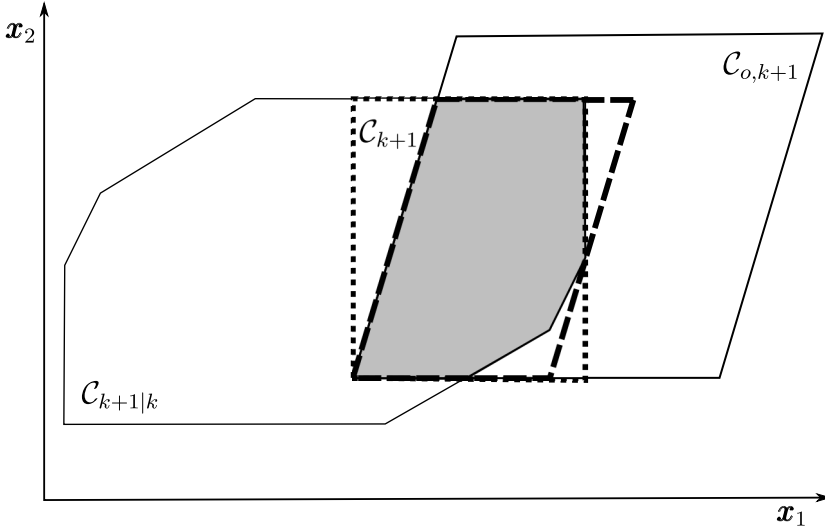


**Figure 3.3:** Example in  $\mathbb{R}^2$  of the update step in a general SSE.

between the propagated set and all the outputs sets. The main goal of the method is to simplify the complexity of the operations in the update step of the SSE but increasing the number of operations to perform. The output sets in this method can be described as  $\mathcal{C}_{o,k}^j \forall j \in [1, n_o]$  where  $j$  depicts the output set of the form 3.20 according to the output  $j$ . Hence, the sequential method can be summarized as,

$$\mathcal{C}_k = \overline{\left( \overline{\left( \left( \overline{\left( \mathcal{C}_{k|k-1} \cap \mathcal{C}_{o,k}^1 \right)} \cap \mathcal{C}_{o,k}^2 \right)} \cdots \cap \mathcal{C}_{o,k}^{n_o} \right)} \right)}, \quad (3.21)$$

where  $\overline{(\cdot)}$  represents an outbounding operation (a reminder that this is an over-approximation of the intersection). The order of the intersections can be adjusted based on user's experience. In general, this method is easier to develop but implies less accuracy.

### 3.2.2.2 Block Approach

The key idea behind this method lies in developing a unique output set with the available outputs, taking into account all their particular bounds. The construction of this set is in general trivial. However, the set is more complex (in terms of facets) than taking only one output, hence, the intersection step (the outer out-bounded set)

implies at least, an increment in the computational cost. This method is recommended for SSE approaches where the reduction of the set complexity is given in additional steps.

### 3.3 Set-Membership State Estimation with Parallelotopes

The foundations of SSE using parallelotope were given by Vicino and Zappa [31] and Chisci et al. [11]. A Recursive Optimal Parallelotope Outbounding (better known as ROPO) was developed for one [31] or multiple outputs, [11]. ROPO is the parallelotope with the minimum volume that encloses the intersection between the predictive parallelotope and the output set.

The use of parallelotope is widely spread in the SSE. In Ramdani and Poignet [23] was designed a robust dynamic identification comparison of two ellipsoids methods against ROPO approach over a two degrees-of-freedom SCARA robot. Results show that ROPO exhibits a less conservative answer than ellipsoid approaches in all simulations.

Ingimundarson et al. [16] used ROPO for robust fault detection in a quadruple tank process. The authors showed that consistency checks indicating faults can be performed in a natural manner with a parallelotope description of the feasible parameter set.

Alamo et al. [2] used parallelotopes with DC programming to obtain a guaranteed bound of the uncertain trajectory of the nonlinear system each sampling time.

Sharma et al. [27] reported that the parallelotope with the minimum volume was not always the optimal solution under MPC control problems. In this sense, the authors proposed two new improvements to ROPO, one of them prioritized the output set and the second approach prioritized the constraints. Later, Valero and Paulen [29] proposed an algorithm which take into consideration past extreme measurement to reduce the conservativeness in the set. In [30] the same approach is extended to multiple outputs. In this section the latter approach together with the well known ROPO is described.

In all parallelotopic approaches of this section the predictive set is a parallelotope,  $\mathcal{P}_k$  and the output set is a group of strips (that depend on the number of outputs),  $\mathcal{S}_k^i$ . In the ROPO approach only one output is considered. The intersection step is performed between the predictive parallelotope and one strip.

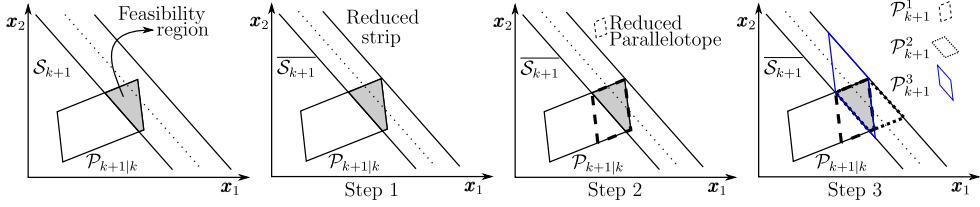


**Figure 3.4:** Illustration of the ROPO algorithm in a two-dimensional state space.

### 3.3.1 Recursive Optimal Parallelotopic Outbounding (ROPO)

The idea behind the ROPO-class algorithms consists in intersecting the output strip and the predicted parallelotope, which bounds all the possible realizations of state variables, and finding the best parallelotope that outbounds the intersection.

The ROPO algorithm finds a parallelotope from the intersection of  $n + 1$  strips. These are given by an output strip  $\mathcal{S}_{k+1} := \mathcal{S}(\mathbf{p}_0, c_0)$  and by a parallelotope  $\mathcal{P}_{k+1|k}(\mathbf{T}_{k+1}, \boldsymbol{\theta}_{c,k+1})$  that predicted at time  $k + 1$  based on a priori state knowledge given by the parallelotope  $\mathcal{P}_k := \mathcal{P}(\mathbf{T}_k, \boldsymbol{\theta}_{c,k})$  at time  $k$ . The prediction is realized as (3.17). To perform this equation is required a linear transformation (See 2.3.2.1) and the Minkowski sum (See 2.3.2.2). However, the last one is avoided by dropping these terms in this approach. Therefore, The simulation cases presented here that use polytopes do not consider these sets.

The algorithm assumes that the direction vectors  $\mathbf{t}_{k+1,i}$  of the parallelotope  $\mathcal{P}_{k+1|k}$  are such that  $\mathbf{p}_0^\top \mathbf{t}_{k+1,i} \geq 0$ ,  $\forall i = \{1, \dots, n\}$ , which represents the projections of the generators  $\mathbf{t}_{k+1,i}$  on the vector  $\mathbf{p}_0$ . This assumption amounts to fixing positive directions along the axes of the parallelotope and requires replacing  $\mathbf{t}_i$  by  $-\mathbf{t}_i$  in  $\mathbf{T}$  for those indices for which this inequality is not satisfied (See Figure 2.6, the column vector of  $\mathbf{T}$ , regardless of the sign it takes, describes the direction of the parallelotope). The ROPO algorithm identifies the minimal-volume parallelotope outbounding  $\mathcal{S}_{k+1} \cap \mathcal{P}_{k+1|k}$  in three steps.

#### 3.3.1.1 Step 1: Tightening the output strip $\mathcal{S}_0$

As the output strip may not completely overlap with  $\mathcal{P}_{k+1|k}$  (as shown in Figure 3.4), a reduced strip  $\bar{\mathcal{S}}_0(\bar{\mathbf{p}}_0, \bar{c}_0)$  is introduced

$$\bar{\mathbf{p}}_0 := \frac{2}{r_0^+ + r_0^-} \mathbf{p}_0 \quad \bar{c}_0 := 1 + \frac{2c_0}{r_0^+ + r_0^-} \quad (3.22)$$

where  $r_0^+ := \min(1, \epsilon_0^+)$  and  $r_0^- := \min(1, -\epsilon_0^-)$  and the scalars  $\epsilon_0^+$  and  $\epsilon_0^-$  are given by

$$\epsilon_0^\pm := (\mathbf{p}_0^\top \boldsymbol{\theta}_{c,k+1} - c_0) \pm \sum_{i=1}^n \mathbf{p}_0^\top \mathbf{t}_{k+1,i} \quad (3.23)$$

### 3.3.1.2 Step 2: Reducing the parallelotope $\mathcal{P}_{k+1|k}$

The reduced parallelotope is constructed to reduce the volume of  $\mathcal{P}_{k+1|k}$ , which is not a part of the intersection between  $\mathcal{P}_{k+1|k} \cap \mathcal{S}_{k+1}$  (see Figure 3.4 step 2). The reduced parallelotope  $\bar{\mathcal{P}}_{k+1|k} := \mathcal{P}(\bar{\mathbf{T}}, \bar{\boldsymbol{\theta}}_c)$  is found according to (for  $i \in \{1, \dots, n\}$ )

$$\bar{\mathbf{t}}_i := \frac{r_i^+ + r_i^-}{2} \mathbf{t}_{k+1,i} \quad (3.24)$$

$$\bar{\boldsymbol{\theta}}_c := \boldsymbol{\theta}_{c,k+1} + \sum_{i=1}^n \frac{r_i^+ - r_i^-}{2} \mathbf{t}_{k+1,i} \quad (3.25)$$

with

$$r_i^\pm := \begin{cases} \min\left(1, \frac{1 \mp \epsilon_0^\mp}{\mathbf{p}_0^\top \mathbf{t}_{k+1,i}} - 1\right), & \text{if } \mathbf{p}_0^\top \mathbf{t}_{k+1,i} \neq 0 \\ 1, & \text{if } \mathbf{p}_0^\top \mathbf{t}_{k+1,i} = 0 \end{cases} \quad (3.26)$$

### 3.3.1.3 Step 3: Selecting the minimal volume parallelotope $\mathcal{P}_{k+1}$

There are  $n + 1$  strips defining the intersection  $\bar{\mathcal{P}}_{k+1|k} \cap \bar{\mathcal{S}}_0$ , unless the output strip is parallel to one of the strips that form  $\mathcal{P}_{k+1}$ . Thus, there are  $n + 1$  possible parallelotopes for outbounding the intersection (see Figure 3.4). The minimum-volume parallelotope is selected by removing the strip  $\mathcal{S}_{i^*}$  with the largest projection on  $\mathbf{p}_0$ . Let us introduce,

$$i^* := \arg \max_{j \in \{0, 1, \dots, n\}} \bar{\mathbf{p}}_0^\top \bar{\mathbf{t}}_j \quad \text{with } \bar{\mathbf{t}}_0 := \bar{\mathbf{p}}_0 / \|\bar{\mathbf{p}}_0\|_2^2 \quad (3.27)$$

The resulting outbounding parallelotope is given by

$$\mathcal{P}_{k+1} := \begin{cases} \bar{\mathcal{P}}_{k+1|k}(\bar{\mathbf{T}}, \bar{\boldsymbol{\theta}}_c), & \text{if } i^* = 0 \\ \mathcal{P}^*(\mathbf{T}^*, \boldsymbol{\theta}_c^*), & \text{otherwise} \end{cases} \quad (3.28a)$$

$$\text{where } \boldsymbol{\theta}_c^* := \bar{\boldsymbol{\theta}}_c + \frac{1}{\bar{\mathbf{p}}_0^\top \bar{\mathbf{t}}_{i^*}} \bar{\mathbf{t}}_{i^*} (\bar{c}_0 - \bar{\mathbf{p}}_0^\top \bar{\boldsymbol{\theta}}_c) \quad (3.28b)$$

$$\mathbf{t}_i^* := \begin{cases} \bar{\mathbf{t}}_i - \frac{\bar{\mathbf{p}}_0^\top \bar{\mathbf{t}}_i}{\bar{\mathbf{p}}_0^\top \bar{\mathbf{t}}_{i^*}} \bar{\mathbf{t}}_{i^*}, & \text{if } i \neq i^* \\ \frac{1}{\bar{\mathbf{p}}_0^\top \bar{\mathbf{t}}_{i^*}} \bar{\mathbf{t}}_{i^*}, & \text{otherwise} \end{cases} \quad (3.28c)$$

A robust control min-max approach with an SSE strategy with ROPO under bounded disturbances without uncertainties in the model is represented in Algorithm 2.

---

**Algorithm 2** Robust control min-max algorithm using ROPO.

---

**Input:**  $\mathcal{P}_k(\mathbf{T}_k, \boldsymbol{\theta}_{c,k}), \mathcal{S}_{k+1}^i, \forall i \in [1, n_o]$

**Initialization:**  $k := 1$

**Main Loop:**

1. Propagate  $\mathcal{P}_k \rightarrow \mathcal{P}_{k+1|k}$  by one time step. This is,
 
$$\mathcal{P}_{k+1|k}(\mathbf{T}_{k+1}, \boldsymbol{\theta}_{c,k+1}) = \{\mathbf{x}_{k+1} = \mathbf{A}\mathbf{T}_k\mathbf{v} + \mathbf{A}\boldsymbol{\theta}_c + \mathbf{B}\mathbf{u}_k, \|\mathbf{v}\|_\infty \leq \mathbf{1}\}.$$
2. **For each**  $i \in [1, n_o]$   
Using  $\mathcal{P}_{k+1|k}$  and  $\mathcal{S}_{k+1}^i$ , apply Equations 3.22 to 3.28.
3. Assign  $\mathcal{P}_{k+1} := \mathcal{P}_{k+1|k}$
4. Find the optimal control input by solving (3.46) with  $\mathcal{P}_{k+1}$ .
5. Apply the control step,  $k = k + 1$ , and go to step 1.

**Output:**  $\mathcal{P}_{k+1}(\mathbf{T}_{k+1}, \boldsymbol{\theta}_{c,k+1})$  and control input  $\mathbf{u}_{k+1}$ .

---

### 3.3.2 Extremal-measurements ROPO

The ROPOe was presented by Valero and Paulen [29]. Later in the same year, [30] showed the multi-output approach for this algorithm. The heuristics-based algorithm relies on the fact that major improvement in the estimation error is brought by the measurements with large innovations. This principle is similar to the introduced by [11]. Overall, ROPOe uses past information to improve the reduction of the feasibility region (current predicted parallelotope). The propagated information can then be used as additional strips to enhance the recursive estimation. For each output, ROPOe is going to employ three different strips for the reduction of the parallelotope: one bearing the information from the current measurement output and the other two strips bearing the information from extremal innovations that propagated (using (2.17)) until the current time.

The criterion for selecting strips (from past) to exploit is selected as the Euclidean distance between the center of the reduced parallelotope and all three strips considered. The strips with the maximum and minimum distance are selected and kept for the next iteration. In each iteration, it is assumed that we have three strips (two from the past and one built with the current measurement output). In the first iteration,

those strips from the past could come from some heuristic or previous knowledge of the plant. In this work, we use the strips from the initial parallelotope. A description of the implementation of this method within an MPC is given in Algorithm 3.

---

**Algorithm 3** MPC with Extremal-measurements ROPO algorithm (ROPOe).

---

**Input:**  $\mathcal{P}_0$ ,  $\mathcal{S}_{+,k-1}^i(\mathbf{p}_+^i, c_+^i) := \mathcal{S}_{-,k-1}^i(\mathbf{p}_-^i, c_-^i), \forall i \in \{0, \dots, m\}$

**Initialization:**  $k := 1$

**Main Loop:**

1. Get output strips  $\mathcal{S}_k^i(\mathbf{p}^i, c^i), \forall i \in \{0, \dots, m\}$ .
  2. Propagate  $\mathcal{P}_{k-1} \rightarrow \mathcal{P}_{k|k-1}$ ,  $\mathcal{S}_{+,k-1}^i \rightarrow \mathcal{S}_{+,k}^i$ , and  $\mathcal{S}_{-,k-1}^i \rightarrow \mathcal{S}_{-,k}^i, \forall i \in \{0, \dots, m\}$  by one time step.
  3. **For each**  $i \in \{0, \dots, m\}$ :  
Use ROPO to update  $\tilde{\mathcal{P}}_k \rightarrow \mathcal{P}_k$  with  $\mathcal{S}_{+,k}^i$ ,  $\mathcal{S}_{-,k}^i$ , and  $\mathcal{S}_k^i$ .
  4. **For each**  $i \in \{0, \dots, m\}$ :
    - (a) Tighten  $\mathcal{S}_{+,k}^i$ ,  $\mathcal{S}_{-,k}^i$  and  $\mathcal{S}_k^i$  with respect to  $\mathcal{P}_k$  through Step 1 of the ROPO algorithm.
    - (b) Set  $e_k := \left( \mathbf{p}_k^{i,\top} \boldsymbol{\theta}_c - c_k^i \right) / \|\mathbf{p}_k^i\|_2$ ,  
 $e_{\pm} := \left( \mathbf{p}_{\pm}^{i,\top} \boldsymbol{\theta}_c - c_{\pm}^i \right) / \|\mathbf{p}_{\pm}^i\|_2$ .
    - (c) Update  $\mathcal{S}_+$  and  $\mathcal{S}_-$  with  
 $p := \arg \max_{j \in k, +, -} e_j$ ,  $\mathcal{S}_+^i(\cdot) := \mathcal{S}_p^i(\mathbf{p}^p, c^p)$ ,  
 $p := \arg \min_{j \in k, +, -} e_j$ ,  $\mathcal{S}_-^i(\cdot) := \mathcal{S}_p^i(\mathbf{p}^p, c^p)$
  5. Find the optimal control input by solving (3.46) with  $\mathcal{P}_k$ .
  6. Apply the first control step,  $k = k + 1$ , and go to step 1.
- 

### 3.3.3 Parallelotope State Estimation for Multi-output Systems

#### 3.3.3.1 Sequential Approach

The sequential approach consists in sequential application of the ROPO algorithm using all  $m$  output strips. This process can be summarized as

$$\mathcal{P}_{k+1} := \overline{\left( \overline{\left( \overline{\left( \mathcal{P}_{k+1} \cap S_1 \right) \cap S_2} \right) \cdots \cap S_m} \right)}, \quad (3.29)$$

where  $\overline{(\cdot)}$  represents an outbounding operation. The order of the intersections can be adjusted based on user's experience.

### 3.3.3.2 Block Approach

In the block approach, the key idea is to process  $m$  new strips (developed by  $m$  outputs with their respective error bounds) simultaneously with the  $n$  strips that form the predicted parallelotope  $\mathcal{P}_{k+1|k}$ . This method requires two steps; tightening the strips and selecting the parallelotope with the minimum volume. The first step is performed by applying *Step 1* and *Step 2* of the ROPO algorithm  $2m - 1$  times. For example with  $m = 2$ , we first tighten the strip  $\mathcal{S}_1(\mathbf{p}_1, c_1)$ , the the strip  $\mathcal{S}_2(\mathbf{p}_2, c_2)$  and finally the strip  $\mathcal{S}_1(\mathbf{p}_1, c_1)$  again. The second step is taken using *Step 3* of the ROPO algorithm across all  $m$  strips and selecting the parallelotope based on the minimum volume using the determinant of the generator matrix as a discriminating index. For developing Block ROPOe, it is necessary to change only the *Step 3* of Algorithm 3. This new step consist in grouping all the strips ( $\mathcal{S}_{+,k}^i, \mathcal{S}_{-,k}^i, \mathcal{S}_k^i, \forall i \in \{0, \dots, m\}$ ) and applying Block ROPO. The rest of the algorithm remains the same.

## 3.4 Set-Membership State Estimation with Polytopes

In order to reduce the conservatism in the control input produced by SSE approaches many strategies have emerged. It is clear that an accurate intersection step will decrease the size of the feasibility region and consequently, the conservatism of the system. This is the reason why Kuntsevich [17] developed an SSE strategy using polytopes. However, the complexity in the resulting polytopes became intractable. Later, Spathopoulos and Grobov [28] tried to solve this problem with linear programming. After this point, to the best of our knowledge no other authors work with polytope (in half-spaces representation) to perform an SSE. Next, we propose a novel non-linear programming (NLP) problem that allows performing an SSE using polytopes.

In this case, uncertainties due to mismatches in the process, as well as, bounded noise in outputs are considered. Uncertainties and measurement bounded noises are enclosed in known polytopes (see Assumption 2). The region where the true value of the system is located, it is also known and enclosed by a polytope (see Assumption 1). This is,

$$\Omega \oplus \Gamma \subseteq \mathbb{P}_\omega(\mathbf{G}_\omega(\mathbf{P}_k), \mathbf{h}_\omega(\mathbf{P}_k)) \quad \Psi \subseteq \mathbb{P}_\nu(\mathbf{G}_\nu, \mathbf{h}_\nu) \quad \text{And} \quad \text{w.l.o.g. } \mathbf{x}_k \in \mathbf{P}_k(\mathbf{G}_k, \mathbf{h}_k) \quad (3.30)$$

where  $\mathbf{G}_\omega(\mathbf{P}_k) \in \mathbb{R}^{n_\omega \times n}$ ,  $\mathbf{h}_\omega(\mathbf{P}_k) \in \mathbb{R}^{n_\omega}$ ,  $\mathbf{G}_\nu \in \mathbb{R}^{2n_o \times n_o}$ ,  $\mathbf{h}_\nu \in \mathbb{R}^{2n_o}$  and finally,  $\mathbf{G}_k \in \mathbb{R}^{m \times n}$ ,  $\mathbf{h}_k \in \mathbb{R}^m$ . At this point, it needs to be mentioned that  $\mathbf{G}_\omega$  and  $\mathbf{h}_\omega$  are, in the most general case, functions dependent of  $\mathbf{P}_k$ , even when the system is assumed invariant and the bounds of  $\Omega$  fixed, the nonlinearity bounds depend on the current state bounds and these to the shape parameters  $\mathbf{G}_k$  and  $\mathbf{h}_k$  of the input polytope.

**Remark 6.** *The output polytope on each step time is built in the following way. The true value of the output of the system is enclosed by,*

$$\mathbf{y}_k = \mathbf{C}\mathbf{x}_k \in \{\mathbf{y}_{m,k} \oplus \mathbf{P}_\nu(\mathbf{G}_\nu, \mathbf{h}_\nu)\} \quad (3.31)$$

We will assume that the elements of  $\mathbf{P}_\nu$  are denoted by  $\mathbf{x}_\nu$ , then, the Minkowski sum is given by,

$$\begin{aligned} \mathbf{y}_k &= \mathbf{y}_{m,k} + \mathbf{x}_\nu \\ \mathbf{x}_\nu &= \mathbf{y}_k - \mathbf{y}_{m,k} \end{aligned}$$

Now, using the polytope definition it gets,

$$\begin{aligned} \mathbf{G}_\nu(\mathbf{y}_k - \mathbf{y}_{m,k}) &\leq \mathbf{h}_\nu \\ \mathbf{G}_\nu\mathbf{y}_k - \mathbf{G}_\nu\mathbf{y}_{m,k} &\leq \mathbf{h}_\nu \\ \mathbf{G}_\nu\mathbf{C}\mathbf{x}_k &\leq \mathbf{h}_\nu + \mathbf{G}_\nu\mathbf{y}_{m,k} \\ &\Rightarrow \mathbf{P}_{o,k}(\mathbf{G}_o, \mathbf{h}_o) \end{aligned}$$

Therefore, the output set for this SSE is given by the polytope  $\mathbf{P}_{o,k}(\mathbf{G}_o, \mathbf{h}_o)$ .

Next, the main idea is to use the polytopic arithmetic rules from Proposition (2.6.4) to recursively construct polytopic outer approximations of the form

$$\mathbf{P}_{k+1}(\mathbf{G}_{k+1}, \mathbf{h}_{k+1}) \supseteq \mathbf{P}_{k+1|k}(\mathbf{G}_{k+1|k}, \mathbf{h}_{k+1|k}) \cap \mathbf{P}_{o,k+1}(\mathbf{G}_{o,k+1}, \mathbf{h}_{o,k+1})$$

where the propagation and update step take the form

$$\mathbf{P}_{k+1|k}(\mathbf{G}_{k+1|k}, \mathbf{h}_{k+1|k}) = (\mathbf{A}\mathbf{P}_k(\mathbf{G}_k, \mathbf{h}_k) + \mathbf{B}\mathbf{u}_k) \oplus \mathbf{P}_\omega(\mathbf{G}_\omega, \mathbf{h}_\omega) \quad (3.32)$$

$$\mathbf{P}_{k+1}(\mathbf{G}_{k+1}, \mathbf{h}_{k+1}) \supseteq \mathbf{P}_{k+1|k} \cap \mathbf{P}_{o,k+1} \quad (3.33)$$

The following theorem outlines a method for the construction of polytopic enclosures for the sets  $\mathbf{P}_k$ .

**Theorem 1.** *Let the matrix  $\mathbf{A}$  be invertible. Hence, for each step time there exist non-negative matrices  $\mathbf{M} \in \mathbb{R}_+^{m \times (m+n_\omega)}$ ,  $\mathbf{N} \in \mathbb{R}_+^{n_\omega \times (m+n_\omega)}$ ,  $\mathbf{\Lambda} \in \mathbb{R}_+^{(m+n_\omega+2n_o) \times \ell}$  that*

produce pairs  $\mathbf{G}_{k+1} \in \mathbb{R}_+^{\ell \times n}$  and  $\mathbf{h}_{k+1} \in \mathbb{R}_+^\ell$ , which satisfy

$$\mathbf{G}_{k+1} = \Lambda^\top \begin{bmatrix} M^\top \mathbf{G}_k \mathbf{A}^{-1} \\ \mathbf{G}_\nu \mathbf{C} \end{bmatrix} \quad (3.34)$$

$$\mathbf{h}_{k+1} = \Lambda^\top \begin{bmatrix} M^\top (\mathbf{h}_k + \mathbf{G}_k \mathbf{A}^{-1} \mathbf{B} \mathbf{u}_k) + N^\top \mathbf{h}_\omega(\mathbf{P}_k) \\ \mathbf{h}_\nu + \mathbf{G}_\nu \mathbf{y}_{m,k+1} \end{bmatrix} \quad (3.35)$$

$$N^\top \mathbf{G}_\omega(\mathbf{P}_k) = M^\top \mathbf{G}_k \mathbf{A}^{-1} \quad (3.36)$$

then we have  $\mathbf{P}_{k+1}(\mathbf{G}_{k+1}, \mathbf{h}_{k+1}) \supseteq \mathbf{P}_{k|k-1} \cap \mathbf{P}_{o,k}$ ,  $\forall k \in \mathbb{N}$ .

**Proof 10.** The proof proceeds by induction. First, notice that the propagation step is given by the Equation (3.32), if we apply the Property (2.6.4.2) and the Minkowski sum condition found in the Equation (2.99) over the propagation step, we get,

$$\mathbf{P}_{k+1|k}(\mathbf{G}_{k+1|k}, \mathbf{h}_{k+1|k}) = (\mathbf{A} \mathbf{P}_k(\mathbf{G}_k, \mathbf{h}_k) + \mathbf{B} \mathbf{u}_k) \oplus \mathbf{P}_\omega(\mathbf{G}_\omega(\mathbf{P}_k), \mathbf{h}_\omega(\mathbf{P}_k)) \quad (3.37)$$

$$= \mathbf{P}(\mathbf{G}_k \mathbf{A}^{-1}, \mathbf{h}_k + \mathbf{G}_k \mathbf{A}^{-1} \mathbf{B} \mathbf{u}_k) \oplus \mathbf{P}_\omega(\mathbf{G}_\omega(\mathbf{P}_k), \mathbf{h}_\omega(\mathbf{P}_k)) \quad (3.38)$$

$$= \mathbf{P}(M^\top \mathbf{G}_k \mathbf{A}^{-1}, M^\top (\mathbf{h}_k + \mathbf{G}_k \mathbf{A}^{-1} \mathbf{B} \mathbf{u}_k) + N^\top \mathbf{h}_\omega(\mathbf{P}_k)) \quad (3.39)$$

with

$$N^\top \mathbf{G}_\omega(\mathbf{P}_k) = M^\top \mathbf{G}_k \mathbf{A}^{-1} \quad (3.40)$$

In the update step, the exact intersection between the predictive polytope and the output polytope by the Property 2.6.4.1 in the following form,

$$\mathbf{P}_{k+1|k} \cap \mathbf{P}_{o,k+1} = \mathbf{P}_\cap(\mathbf{G}_\cap, \mathbf{h}_\cap) \quad (3.41)$$

where Equation (3.40) holds and,

$$\mathbf{G}_\cap = \begin{bmatrix} M^\top \mathbf{G}_k \mathbf{A}^{-1} \\ \mathbf{G}_\nu \mathbf{C} \end{bmatrix} \quad \mathbf{h}_\cap = \begin{bmatrix} M^\top (\mathbf{h}_k + \mathbf{G}_k \mathbf{A}^{-1} \mathbf{B} \mathbf{u}_k) + N^\top \mathbf{h}_\omega(\mathbf{P}_k) \\ \mathbf{h}_\nu + \mathbf{G}_\nu \mathbf{y}_{m,k} \end{bmatrix} \quad (3.42)$$

The exact intersection is not tractable. Therefore, if we apply the facet reduction condition found in the Property 2.6.4.3 over this polytope, we get our theorem. This is,

$$\mathbf{P}_\cap(\mathbf{G}_\cap, \mathbf{h}_\cap) \subset \mathbf{P}_{k+1}(\Lambda^\top \mathbf{G}_\cap, \Lambda^\top \mathbf{h}_\cap) \quad (3.43)$$

when Equation (3.41) holds. Hence, the theorem is demonstrated.

In order to apply the above theorem for constructing enclosures one needs to select matrices  $M_k, N_k$ , and  $\Lambda_k$ . This enclosure selection can be done by computing a minimizer of

$$\min_{\mathbf{G}_k, \mathbf{h}_k, M_k, N_k, \Lambda_k} J(\mathbf{P}(\mathbf{G}_k, \mathbf{h}_k)) \quad \text{s.t.} \quad (\mathbf{G}_k, \mathbf{h}_k) \in \mathbb{G}_k,$$

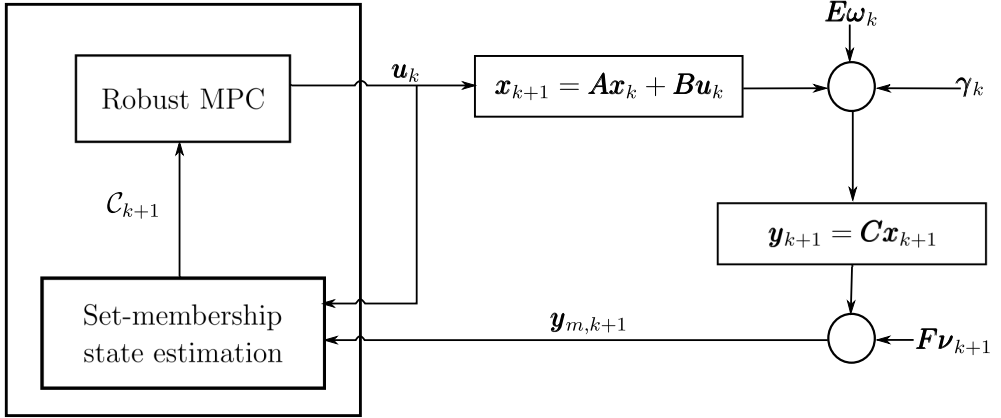


**Figure 3.5:** Robust MPC using set-membership state estimation.

where  $\mathbb{G}_k$  denotes the feasible set of (3.34)–(3.36). In this context,  $J : 2^{\mathbb{R}^n} \rightarrow \mathbb{R}$  is a set-valued function that measures the size of a set  $X \subseteq \mathbb{R}^{n_x}$ . For example, one can minimize the size of the bounding box of  $X$ , i.e.

$$J(X) = \sum_{i=1}^n \sigma[X](e_i) + \sum_{i=1}^n \sigma[X](-e_i)$$

where  $e_i \in \mathbb{R}^n$  is the  $i$ -th standard basis vector of  $\mathbb{R}^n$  and  $\sigma[X]$  the support function of  $X$ . By using standard reformulations based on convex duality for linear programs.

### 3.5 Robust MPC using SSE

SSE guarantees robustness in the observation of the states because it takes into consideration all possible trajectories owing to uncertainties and nonlinearities. Many robust control structures have been developed to use the advantages of SSE and produce a robust control input. This section describes a robust MPC strategy.

A robust MPC refers to hold stability and performance specifications for a specific range of model variations and noise signals. There are different ways to formulate an MPC problem with an estimate of the current state given by a set. We will assume that the cost function is convex. Therefore, we use the min-max MPC [6] approach, where one minimizes the objective function for the worst-case uncertainty realization but which satisfies the plant constraints for any realization. The overall control strategy in the presence of uncertain initial conditions but enclosed in a convex set  $\mathcal{C}_k$ , with

bounded uncertainties in the process  $\omega_k$  and bounded measurement error  $\nu_{k+1}$  is shown in Figure 3.5. The robust control input for polyhedrons is determined by the worst possible state which must lie in one of the vertices of the convex set. Therefore, in this strategy, the computation of the vertices is required.

In the time step  $k = 0$ , the min-max MPC is solved considering all initial conditions given by the vertices of  $\mathcal{C}_0$  and the first control input is applied to the plant. Once the plant measurements are available,  $\mathcal{C}_k$  is computed based on the choice of the set-membership technique chosen. This procedure is repeated until the end. In mathematical terms it can be expressed as,

Given  $\mathcal{C}_k \ni \mathbf{x}_k$ , the min-max MPC solves the problem

$$\min_{\mathbf{u}_i, i \in \mathbb{I}_i} \max_{j \in \mathbb{I}_j} \sum_{i=k}^{k+N_p} J(\mathbf{x}_{i+1}^j, \mathbf{u}_i), \quad (3.44)$$

$$\text{s.t.} \quad \begin{cases} \forall i \in \mathbb{I}_i & \mathbf{x}_{i+1}^j = \mathbf{A}\mathbf{x}_i^j + \mathbf{B}\mathbf{u}_i + \mathbf{E}\Omega + \mathbf{\Gamma}_i^j, \mathbf{x}_k^j = \mathbf{v}_j, \\ \forall j \in \mathbb{I}_j & \mathbf{x}_{i+1}^j \in \mathcal{X}, \mathbf{u}_i \in \mathcal{U}, \end{cases} \quad (3.45)$$

where  $\mathbb{I}_i := \{k, \dots, N_p + k\}$  and  $\mathbb{I}_j$  is an index set of the number of vertices (For the vertex computation of parallelotopes see Algorithm 1). The sets  $\mathcal{X}$  and  $\mathcal{U}$  represent the state and input constraints, respectively.

Due to the convexity of the set of all possible evolutions of the plant along the prediction horizon lies in the set  $\{\mathbf{x}_i^j | j \in \mathbb{I}_j\}$  [25], where  $\mathbf{x}_i^j$  represents the vertex of  $\mathcal{C}_i, \forall i \in \mathbb{I}_i$ . This property ensures the robustness of the calculated control actions  $\mathbf{u}_k$ . To avoid the bi-level optimization, the problem (3.44) can be transformed using the epigraph reformulation with additional inequality constraints [20] as

$$\min_{\mathbf{u}_i, \forall i} \Psi \quad (3.46a)$$

$$\text{s.t.} \quad \sum_{i=k}^{k+N_p} J(\mathbf{x}_{i+1}^j, \mathbf{u}_i) \leq \Psi, \quad \forall i \in \mathbb{I}_i, \forall j \in \mathbb{I}_j, \quad (3.46b)$$

$$\begin{cases} \mathbf{x}_{i+1}^j = \mathbf{A}\mathbf{x}_i^j + \mathbf{B}\mathbf{u}_i + \boldsymbol{\eta}_i^j, \mathbf{x}_k^j = \mathbf{v}_j, \\ \mathbf{x}_{i+1}^j \in \mathcal{X}, \mathbf{u}_i \in \mathcal{U}, \end{cases} \quad (3.46c)$$

## Simulation Studies

---

This chapter discusses three simulation case studies based on linear dynamic systems, for evaluating the concepts discussed in the previous chapters. The case studies are built in MATLAB version R2019b and for the optimization problem the MATLAB toolbox YALMIP has been used [21]. The model for the optimization problem is created once, before starting the simulation, in terms of the variable and the constants in the case study. The overall purpose and set-up of each case study is summarized below.

- Case 1** A double integrator system with uncertain initial conditions is used to perform an SSE using parallelotope, where the ROPO and ROPOe approaches are used to compute a robust MPC control to track the ground reference. In this case, a single input single output (SISO) system is considered. The measurement output is corrupted by a bounded noise.
- Case 2** An extension of the case 1 is performed here. It is a double integrator system with uncertain initial conditions and two outputs corrupted by bounded noises. A block and sequential approaches have been used for ROPO and ROPOe.
- Case 3** A brief comparison between a parallelotopic and polytopic approach without uncertainties in the process over a SISO double integrator system is carried out. The measurement output is corrupted by a bounded noise.
- Case 4** A double integrator system with uncertain initial conditions is used to perform an SSE using polytopes. In this case, states are not linear, but the nonlinearity is bounded to a known polytope. Besides, the measurement output is corrupted by bounded noise.

## 4.1 Case 1. SSE using Parallelotope for SISO system

We test the ROPO and ROPOe methods on the double-integrator example from [27]. The process is given as in (3.15) and (3.16) with

$$\mathbf{A} := \begin{bmatrix} 1 & 1 \\ 0 & 1 \end{bmatrix} \quad \mathbf{B} := \begin{bmatrix} 0 \\ 1 \end{bmatrix} \quad \mathbf{E} = \boldsymbol{\eta} := \begin{bmatrix} 0 \\ 0 \end{bmatrix} \quad \mathbf{C} := [1 \quad 0] \quad \mathbf{F} := 1 \quad (4.1)$$

and with a constraint  $x_1 \geq 0$ , where the states  $x_1$  and  $x_2$  represent the position and the velocity of an object, respectively. The input  $u$  represents object's acceleration at time  $k$ . The initial state vector  $\mathbf{x}_0 := (x_{1,0}, x_{2,0})^\top$ , unknown to both the estimator and the MPC controller, is  $(20, 0)^\top$ . The matrix  $\mathbf{C}$  depicts the measurement of the position and velocity at a sampling rate of 1 s and the measurement error is given with upper bound  $\epsilon = 1$ . The constraints on the input are  $u \in [-1, 1]$ .

The control objective is to steer the object to position zero with zero velocity, which is represented by a stage cost of the MPC controller (3.44) with  $\mathbf{Q} = \mathbf{I}$  and  $\mathbf{R} = 10^{-6}$ . For the problem (3.45), we choose  $N_p = 10$  and  $N_u = 5$  as the prediction horizon and control prediction, respectively.

The cumulative cost  $\text{PI}(k) = \sum_{i=1}^k \mathbf{x}_i^\top \mathbf{x}_i$  is used as a performance index for comparing the estimation concepts. The uncertainty in both the initial states is assumed to be  $\pm 2$ . For the simulations, the initial parallelotopic set  $\mathcal{P}_0$  is selected as

$$\mathcal{P}_0 := \left\{ \begin{bmatrix} 2 & 0 \\ 0 & 2 \end{bmatrix} \mathbf{v} + \begin{bmatrix} 21 \\ 1 \end{bmatrix} \mid \|\mathbf{v}\|_\infty \leq 1 \right\} \quad (4.2)$$

We perform simulations with 10 different realizations of the measurement noise taken from a uniform distribution  $\epsilon_k \sim \mathcal{U}(-1, 1), \forall k$ . The comparison of performance of the presented methods is always carried out using the same error realization.

### 4.1.1 Results

In the simulated closed-loop experiments, the min-max MPC controller with any of the presented state-estimation approaches was able to effectively track the origin. In Figure 4.1, we present the bounds on  $x_1$  given by  $\mathcal{P}_k$ , the evolution of plant's states  $x_1$ , and state  $x_2$  averaged over the considered realizations of measurement error. While the state plots give the feeling about the performance, the bounds of the constrained variable reveal the relation between performance of the estimator and of the controller. Simply speaking, tighter the bounds, better the performance. The worst performance

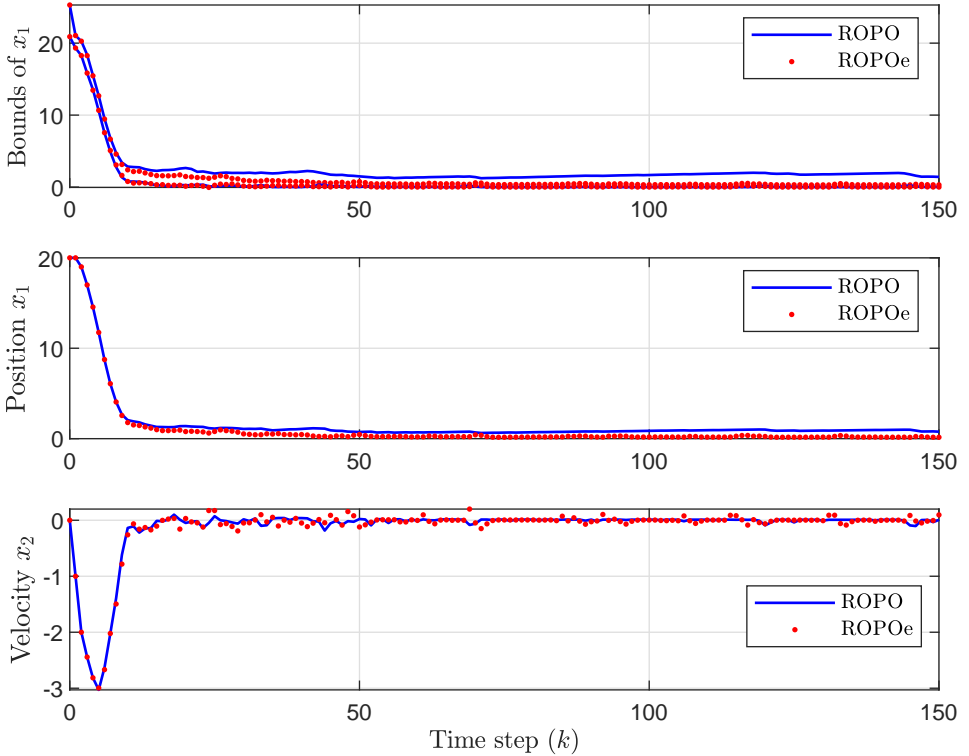


**Figure 4.1:** Bounds on  $x_1$  (top), closed-loop evolution of  $x_1$  (middle), and  $x_2$  (bottom).

is observed for MPC with ROPO algorithm. This is expected since, as discussed earlier and reported by [27], the algorithm might use an outbounding parallelotope that is skewed along one of its axes. The performance of the proposed extremal-measurements-based modification of the ROPO algorithm (ROPOe) is clearly superior compared to ROPO. As it is based on measurement information, the biggest improvement is naturally obtained the measured state  $x_1$ .

Similar conclusions can be drawn from Figure 4.2, which shows cumulative performance of the robust min-max MPC with the presented estimation approaches averaged over 10 realizations of measurement error. The plot shows the time evolution and the bottom one presents statistics (mean and standard deviation) of the cumulative

performance at time 150 s. It is clear that MPC with ROPO estimator achieves the worst performance as measured by both mean performance and its standard deviation. The proposed algorithms achieve superior performance compared to ROPO algorithm.

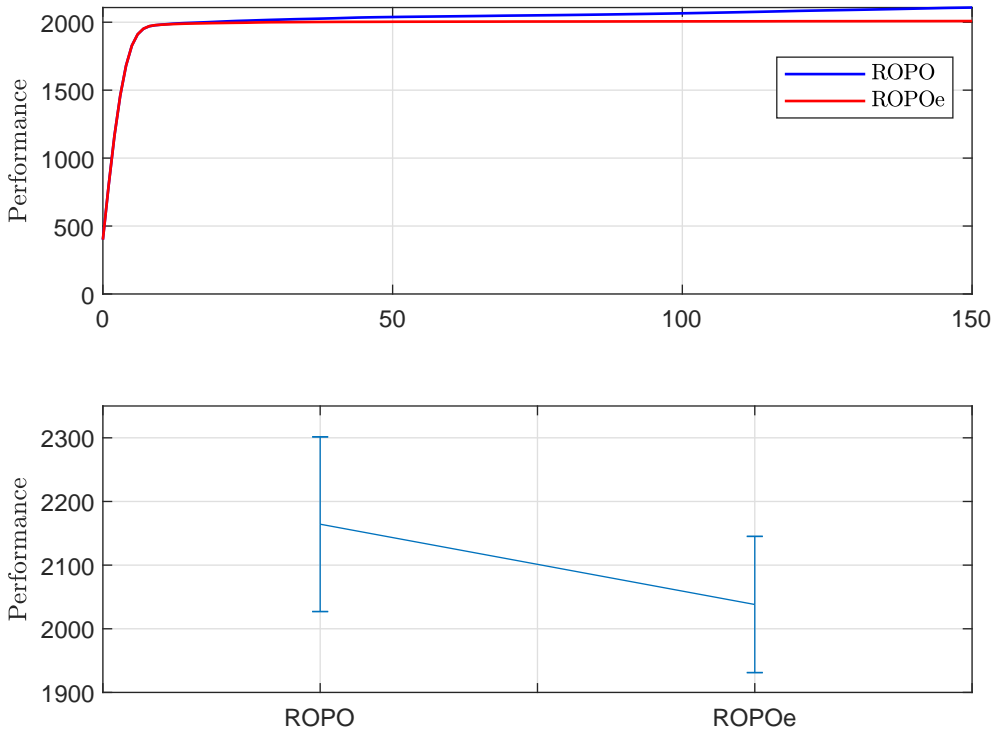


**Figure 4.2:** Cumulative performance of min-max MPC under all studied approaches averaged over 10 different realizations of measurement noise over time (top) and at time 150 s with standard deviations (bottom).

The performance achieved with the ROPOe algorithm is good on average, although its standard deviation is relatively high, which can be attributed to heuristics nature of the algorithm.

In our computational experience, ROPO and ROPOe algorithms exhibit roughly the same CPU time (within 0.001 s). Even though ROPOe algorithm implies several runs of the ROPO algorithm, the increase in CPU time is insignificant in this case.

## 4.2 Case 2. SSE using Parallelotopes for SIMO system

In this case, a similar configuration than the previous case is considered. We test two versions of ROPO and ROPOe methods (Sequential and block approaches) on the double-integrator example. The process is given as in (4.1) with the exception of the output equation, which is given by,

$$\mathbf{C} := \begin{bmatrix} 1 & 0 \\ 0 & 1 \end{bmatrix} \quad \mathbf{F} := \begin{bmatrix} 1 \\ 1 \end{bmatrix} \quad (4.3)$$

Regarding the constraints in the states and control input, as well as, the value of the initial state and the objective of the optimization problem are the same as in the previous case.

### 4.2.1 Results

Figure 4.3 presents the results obtained with min-max MPC using different estimation methods for both the tracked states of the plant and it also shows the respective control inputs. These results are shown for one selected representative realization of the measurement noise out of the performed simulations for the period of 150s. The names of the estimation algorithms are abbreviated as: ROPO with sequential approach (ROPOSeq), ROPO with block approach (ROPOBlock), ROPOe with sequential approach (ROPOeSeq), and ROPOe with block approach (ROPOeBlock). Position reference is not completely reached for any of the presented controllers. This is expected since the position reference collides with the constraint  $x_1 \geq 0$ . This means that if we want to satisfy the constraint robustly, the worst-case (lowest) position has to satisfy it. As shown further, the lowest position satisfies the constraint almost exactly. The tracking of velocity, contrary to the tracking of position, is very good. We can conclude that the controller reaches its design goals.

The performance of the tested estimation algorithms is very similar for the first 50s and all the methods are capable of reducing the uncertainty in the values of the state variables. After the first 50s, the tracking of position is clearly different. Here we can assess the performance of the algorithms and see that this one is significantly better when using the block approach and when using ROPOe approach. Combined approach (ROPOeBlock) is clearly the best.

A recurrent behavior of the response of the robust MPC using parallelotopic estimation is the occurrence of small jumps for all the states and control inputs (see Figure 4.3).

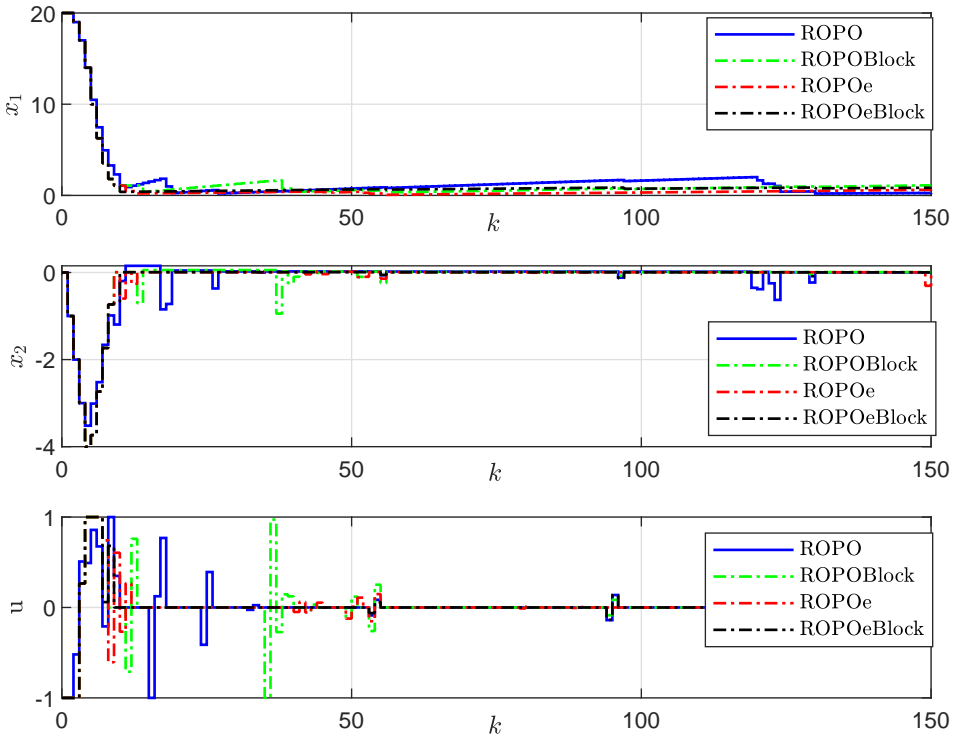


**Figure 4.3:** Evolution of state variables and control inputs over 150s for a selected representative noise realization.

It is important to notice that these jumps are present, however, because the final graphs are taken from the average of all realizations, these can not be appreciated. The jump behavior can be attributed to two factors: 1) From one time step to another, the worst-case vertex of the prediction parallelotope can change, e.g., as a result of the estimation procedure reducing the parallelotope with worst-case scenario. 2) The ROPO algorithm is known to be prone to skew the prediction parallelotope, so that the state bounds can be gradually growing in one direction and be suddenly cut by the measurement strip with a certain realization of the measurement error.

We can confirm the previous observations while seeing Figure 4.4, which shows the bounds of the states that are taken as the minimum/maximum values of the vertices

of the prediction parallelepiped. First, we can see that the lower bound on  $x_1$  clearly saturates the constraint  $x_1$ , which is the reason for plant state  $x_1$  not reaching the reference. Secondly, we can see that the dramatic change of bounds (discussed in the previous paragraph) coincides with the jumps in control inputs and, naturally, with state values. Finally, we can conclude that the estimation performance of the ROPOeBlock algorithm is superior but the performance of ROPOBlock is also very good. While the state and input plots give the feeling about the performance, the bounds of the state variables reveal the relation between performance of the estimator and of the controller. Simply speaking, tighter the bounds, better the performance.

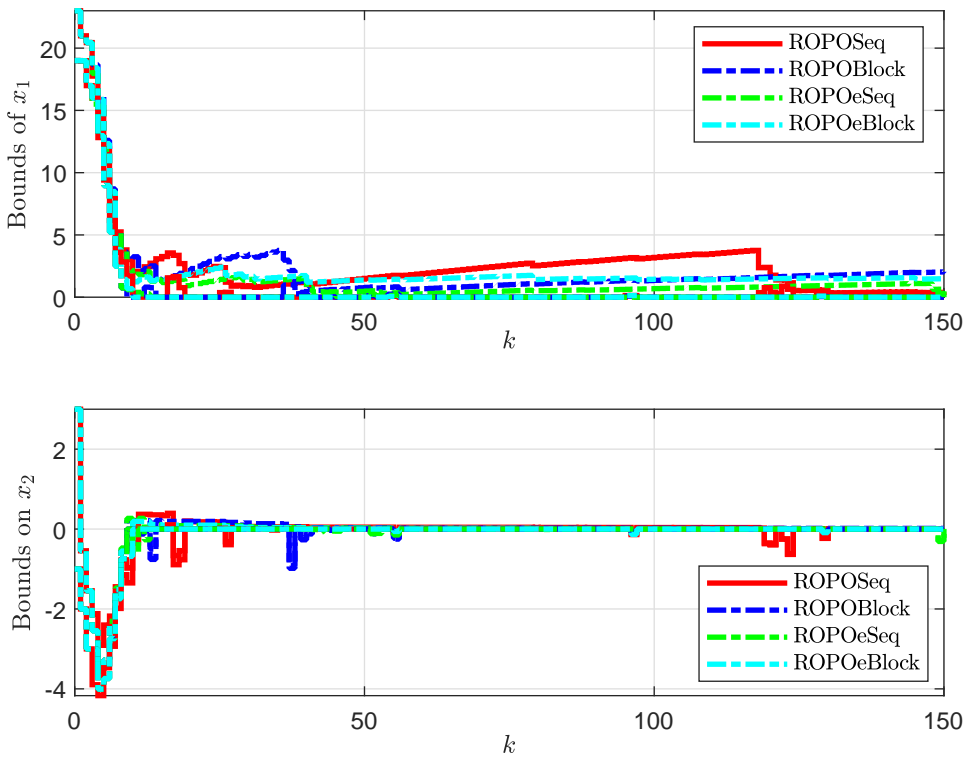


**Figure 4.4:** Evolution of bounds on the state variables over 150s for a selected representative noise realization.

We finally show statistics of the control performance of the presented approaches in

Figure 4.5 (the performance, in this case, is much better than the first case because of the introduction of a second output). Min-max MPC with ROPOeBlock shows the best performance overall. On average, the cumulative cost at 150s is lower than (the second best approach) ROPOBlock by more than 15%, by more than 35% w.r.t. ROPOSeq and by about 40% w.r.t. the ROPO approach. The variances of the performance of these approaches are almost the same (notice the outliers in ROPO case).

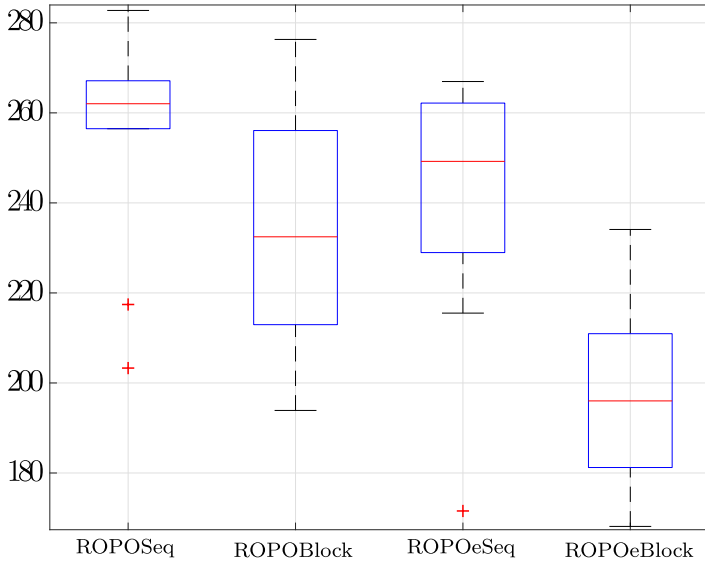


**Figure 4.5:** Boxplots with statistics (first quartile, median, and third quartile) of the control performance reached over 10 different realizations of error.

### 4.3 Case 3. Comparison Between Parallelotopes and Polytopes under SSE

The double integrator is used to show the difference between a parallelotopic and a polytopic approach. The system presents only constraints in the control input  $u \in [-1, 1]$ , and the setup is given as in (3.15) and (3.16) with matrices as (4.1). The system tracks the ground using a general LQR configuration with  $\mathbf{k} = [0.0795 \ 0.4481]^T$ . Hence, only the process of SSE is considered. The true value of the system at  $k = 0$ ,

$x_0 = [19 \ 1]^\top$ , is unknown for the methods but enclosed in a known set given by,

$$\mathcal{P}_0 := \left\{ \begin{bmatrix} 2 & 0 \\ 0 & 2 \end{bmatrix} \mathbf{v} + \begin{bmatrix} 20 \\ 0 \end{bmatrix} \mid \|\mathbf{v}\|_\infty \leq 1 \right\} \quad \mathbf{P}_0 = \begin{pmatrix} 1 & 0 \\ 0 & 1 \\ -1 & 0 \\ 0 & -1 \end{pmatrix} x \leq \begin{pmatrix} 22 \\ 2 \\ -18 \\ 2 \end{pmatrix}. \quad (4.4)$$

The main goal of this case is to show the needs of polytopes for more accurate results. We are going to compare the estimation produced by ROPOe approach against the methodology presented in section 3.4.

### 4.3.1 Results

Figure 4.6 shows the resulting reachable set found by the polytopic and parallelotopic approach. Both methods start with the same set a parallelotope centered in  $[20 \ 0]^\top$  and from the beginning the polytope approach shows important reductions. Actually, the set tends to an element set when  $k$  goes to infinity. Even when the parallelotope tends to decrease over time, the polytope approach is much superior.

## 4.4 Case 4. SSE using Polytopes for SISO system

The double integrator system is studied in the context of bounded-error (set-membership) SSE using the methodology presented in section 3.4. The process is given as in (3.15) and (3.16) with

$$\mathbf{A} := \begin{bmatrix} 1 & 1 \\ 0 & 1 \end{bmatrix} \quad \mathbf{B} := \begin{bmatrix} 0 \\ 1 \end{bmatrix} \quad \mathbf{C} := [1 \ 0] \quad \mathbf{E} := \begin{bmatrix} 1 & 0 \\ 0 & 1 \end{bmatrix} \quad \mathbf{F} := 1 \quad (4.5)$$

where the states  $x_1$  and  $x_2$  represent the position and the velocity of an object, respectively. Both states are subject to bounded uncertainties  $\pm 1$ . The input  $u$  depicts object's acceleration at time  $k$ . It is determined by a discrete LQR controller with  $Q = I$  and  $R = 1$ , saturated at the control bounds  $u \in [-1, 1]$ . The initial state vector is  $x_0 := (20, 10)^\top$ . The output matrix  $\mathbf{C} := [1 \ 0]$  depicts the measurement of the position at a sampling rate of 1 time unit and the uniformly distributed measurement error is bounded in  $\pm 1$ . For the simulations, the initial polytopic set  $\mathbf{P}_0$  is selected such that it includes the true state. The initial polytope is represented as

$$\mathbf{P}_0 = \begin{pmatrix} 1 & 0 \\ 0 & 1 \\ -1 & 0 \\ 0 & -1 \end{pmatrix} x \leq \begin{pmatrix} 32 \\ 11 \\ -15 \\ -6 \end{pmatrix}. \quad (4.6)$$

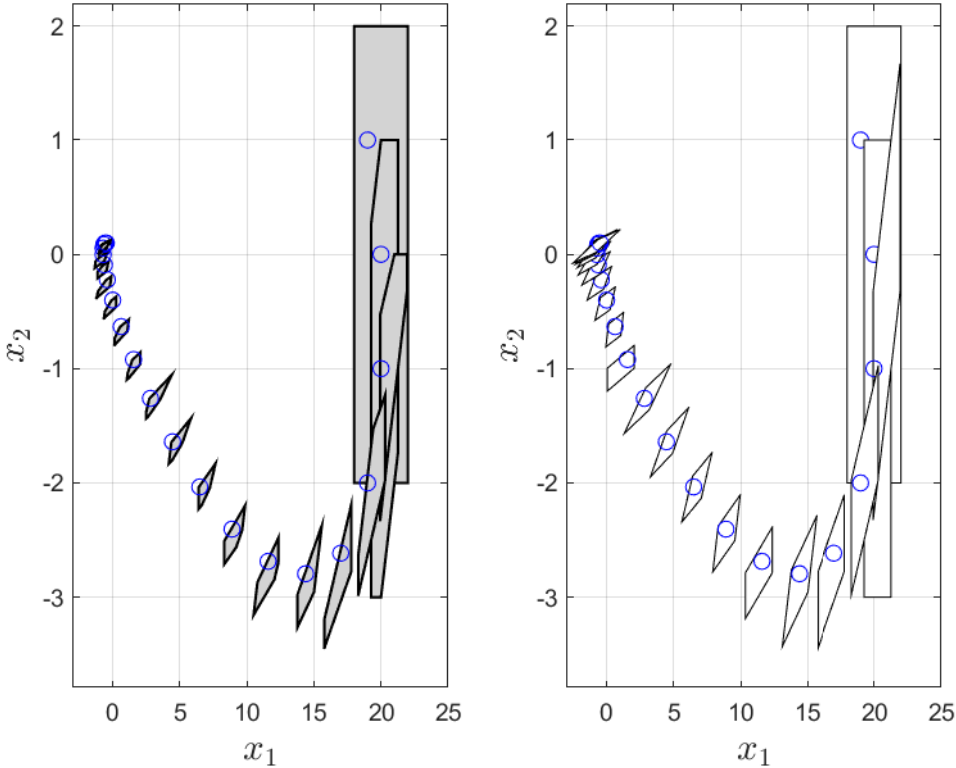


**Figure 4.6:** Polytopic(left) and parallelotopic(right) estimates found for 20 time steps.

#### 4.4.1 Implementation Details

The proposed algorithm is implemented in Matlab using BARON as a global solver and *fmincon*, IPOPT [33] interfaced through OPTI toolbox [13] and YALMIP [21]. Results were graphed using MPT toolbox [15]. We use the global solver to identify a feasible point of (3.4). Local solvers are used afterwards to improve this solution. The process and measurement noises are simulated as random numbers with uniform distributions.

#### 4.4.2 Results

Figure 4.7 shows the reachable set obtained in each iteration. As can be seen, the initial polytope (i.e., a box) contains the initial state,  $(20, 10)^\top$ . At the first time step,

the polytope is considerably reduced due to the difference between the size of the initial polytope and magnitude of the measurement noise. Our computational experience shows that it is not always possible to find the global solution. This gives rise to the non-uniform sizes of the obtained polytopes and certain over-approximations. Our future work will involve a development of sophisticated initialization strategies to obtain consistent state estimation bounds. Figure 4.8 shows the true states against

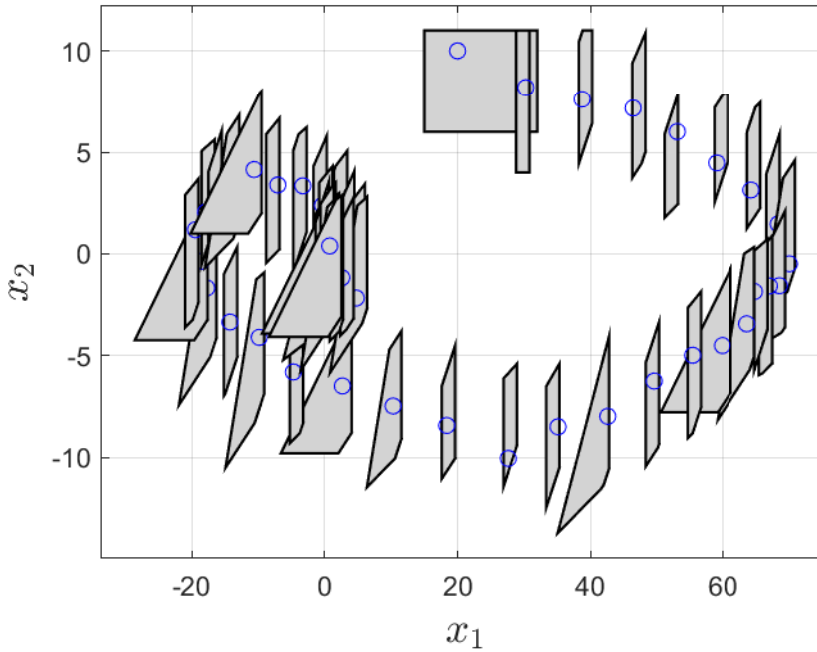


**Figure 4.7:** Polytopic estimates found for 50 time steps.

the bounds (extremal vertices of the polytopic estimates) and the point-prediction of the states (the Chebyshev center of the polytope). We can notice a favorable evolution of the point-prediction towards the true state values. We can also see that despite a large process noise, the estimation procedure is able to maintain the estimation bounds within almost constant range. On some occasions there are jumps occurring in the bounds. These jumps are explained by the inability to identify the global solution of the problem (3.4).

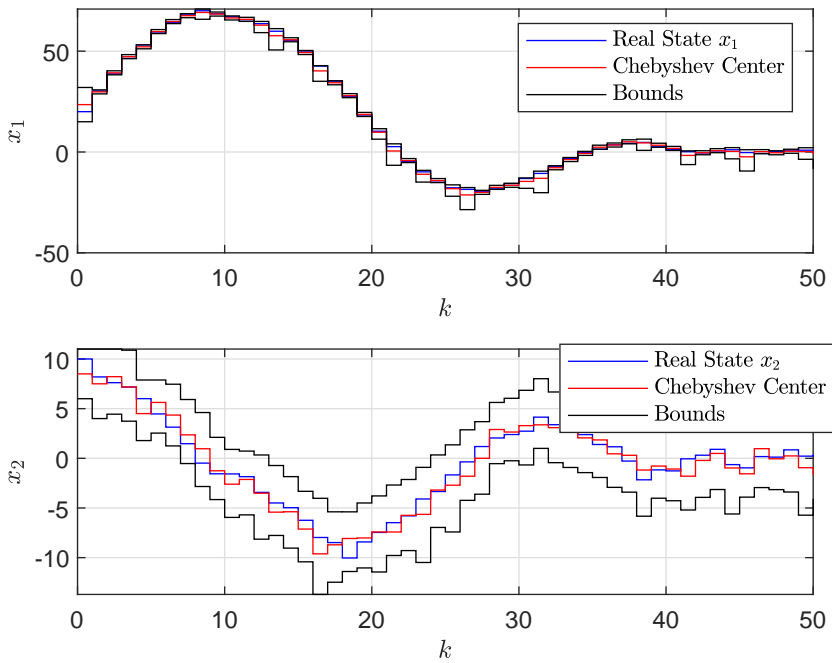


**Figure 4.8:** Evolution of states, their bounds and a Chebyshev center of the bounding polytope.

## Conclusions

---

This mini-thesis summarizes the convex set theory concerning the SSE. The most important sets are defined along with their operations and properties. In most cases, proof of each operation or property is given. A new property for the Minkowski sum of polytope has been found and can also be used for facet reduction in polytopes. A formula for an over-approximation of a parallelotope intersection is provided. Furthermore, it is combined the robust min-max model predictive control with SSE, considering systems with uncertainties in initial conditions under hard input and state constraints.

This mini-thesis led to some new contributions in the area of set-membership state estimation for linear systems: first, a heuristic algorithm that reduces the conservativeness of the predictive parallelotope using strips from the past with extremal realizations is introduced. This algorithm is tested and compared with the ROPO algorithm (developed by Vicino and Zappa [31]) using a double integrator as a benchmark plant for its easy and well known dynamic. Second, it has presented a non-linear program (NLP) able to perform all steps of an SSE scheme using polytopes, this NLP shows directions in a future less expensive and more accurate SSE. Once more, this technique is tested with the double integrator and demonstrates its validity although preliminaries results have not found a formal method to initialize the NLP.

Future works will focus on two research lines. Theory of SSE, in this context, we want to keep working on the computation of Minkowski sum and facet reduction of polytopes, to carry out this task, we plan to use as resulting facet matrix in the Minkowski sum, the intersection facet matrix of the same polytopes, in the case of polytopes in  $\mathbb{R}^2$  is a natural guess. However, in the case of the facet reduction matrix, two possible paths are opened, we can add a new condition in the optimization problem that guarantee minimum volume or we can design a method to initialize this facet matrix.

In addition, we plan a new method for the zonotope order reduction problem; we

plan to follow the principles of Althoff [3] because we notice through simple examples in  $\mathbb{R}^2$  that if we rotate the generator matrix, and after performing the interval hull and we rotate back the same degrees, we can get the zonotope order one with the minimum volume that enclosed the first zonotope. The idea is to extend this principle in  $\mathbb{R}^n$ . Finally, the implementation of SSE approaches. In this sense, we want to apply our strategies in high order systems and nonlinear dynamics with the final aims of developing a completed and simple handbook on SSE for future researchers.

# Bibliography

---

- [1] Alamo, T., Bravo, J. M., and Camacho, E. F. (2005). Guaranteed state estimation by zonotopes. *Automatica*, 41(6):1035–1043.
- [2] Alamo, T., Bravo, J. M., Redondo, M. J., and Camacho, E. F. (2008). A set-membership state estimation algorithm based on dc programming. *Automatica*, 44(1):216–224.
- [3] Althoff, M. (2015). An introduction to cora 2015. In *Proc. of the Workshop on Applied Verification for Continuous and Hybrid Systems*.
- [4] Althoff, M., Stursberg, O., and Buss, M. (2010). Computing reachable sets of hybrid systems using a combination of zonotopes and polytopes. *Nonlinear analysis: hybrid systems*, 4(2):233–249.
- [5] Baotic, M. (2009). Polytopic computations in constrained optimal control. *Automatika*, 50(3-4):119–134.
- [6] Bemporad, A. and Morari, M. (1999). Robust model predictive control: A survey. In *Robustness in identification and control*, pages 207–226. Springer.
- [7] Bertsekas, D. and Rhodes, I. (1971). Recursive state estimation for a set-membership description of uncertainty. *IEEE Transactions on Automatic Control*, 16(2):117–128.
- [8] Blanchini, F. and Miani, S. (2008). *Set-theoretic methods in control*. Springer.
- [9] Boyd, S. and Vandenberghe, L. (2004). *Convex optimization*. Cambridge university press.
- [10] Chabane, S. B., Maniu, C. S., Alamo, T., Camacho, E. F., and Dumur, D. (2014). A new approach for guaranteed ellipsoidal state estimation. *IFAC Proceedings Volumes*, 47(3):6533–6538.
- [11] Chisci, L., Garulli, A., Vicino, A., and Zappa, G. (1998). Block recursive parallelotopic bounding in set membership identification. *Automatica*, 34(1):15 – 22.
- [12] Combastel, C. (2003). A state bounding observer based on zonotopes. In *2003 European Control Conference (ECC)*, pages 2589–2594. IEEE.

- [13] Currie, J. and Wilson, D. I. (2012). OPTI: Lowering the Barrier Between Open Source Optimizers and the Industrial MATLAB User. In Sahinidis, N. and Pinto, J., editors, *Foundations of Computer-Aided Process Operations*, Savannah, Georgia, USA.
- [14] Girard, A. (2005). Reachability of uncertain linear systems using zonotopes. In *International Workshop on Hybrid Systems: Computation and Control*, pages 291–305. Springer.
- [15] Herceg, M., Kvasnica, M., Jones, C., and Morari, M. (2013). Multi-Parametric Toolbox 3.0. In *Proc. of the European Control Conference*, pages 502–510, Zürich, Switzerland. <http://control.ee.ethz.ch/~mpt>.
- [16] Ingimundarson, A., Bravo, J. M., Puig, V., and Alamo, T. (2005). Robust fault diagnosis using parallelotope-based set-membership consistency tests. In *Proceedings of the 44th IEEE Conference on Decision and Control*, pages 993–998. IEEE.
- [17] Kuntsevich, V. (1992). Adaptation and robustness in control systems. *International journal of adaptive control and signal processing*, 6(3):173–182.
- [18] Kurzhanski, A. B. and Varaiya, P. (2000). Ellipsoidal techniques for reachability analysis: internal approximation. *Systems & control letters*, 41(3):201–211.
- [19] Le, V. T. H., Stoica, C., Alamo, T., Camacho, E. F., and Dumur, D. (2013). *Zonotopes: From guaranteed state-estimation to control*. John Wiley & Sons.
- [20] Lofberg, J. (2003). Approximations of closed-loop minimax mpc. In *Proceedings. 42nd IEEE Conference on Decision and Control, 2003.*, volume 2, pages 1438–1442. IEEE.
- [21] Löfberg, J. (2004). Yalmip : A toolbox for modeling and optimization in matlab. In *In Proceedings of the CACSD Conference*, Taipei, Taiwan.
- [22] Merhy, D., Maniu, C. S., Alamo, T., and Camacho, E. F. (2019). Ellipsoidal set-membership state estimation for descriptor systems. In *2019 23rd International Conference on System Theory, Control and Computing (ICSTCC)*, pages 1–6. IEEE.
- [23] Ramdani, N. and Poignet, P. (2005). Robust dynamic experimental identification of robots with set membership uncertainty. *IEEE/ASME Transactions on Mechatronics*, 10(2):253–256.
- [24] Rego, B. S., Raffo, G. V., Scott, J. K., and Raimondo, D. M. (2020). Guaranteed methods based on constrained zonotopes for set-valued state estimation of nonlinear discrete-time systems. *Automatica*, 111:108614.

- 
- [25] Scokaert, P. O. and Mayne, D. (1998). Min-max feedback model predictive control for constrained linear systems. *IEEE Transactions on Automatic control*, 43(8):1136–1142.
- [26] Scott, J. K., Raimondo, D. M., Marseglia, G. R., and Braatz, R. D. (2016). Constrained zonotopes: A new tool for set-based estimation and fault detection. *Automatica*, 69:126–136.
- [27] Sharma, U., Thangavel, S., Mukkula, A. R. G., and Paulen, R. (2018). Effective recursive parallelotopic bounding for robust output-feedback control. *IFAC-PapersOnLine*, 51(15):1032–1037.
- [28] Spathopoulos, M. and Grobov, I. (1996). A state-set estimation algorithm for linear systems in the presence of bounded disturbances. *International Journal of Control*, 63(4):799–811.
- [29] Valero, C. E. and Paulen, R. (2019a). Effective recursive set-membership state estimation for robust linear mpc. *IFAC-PapersOnLine*, 52(1):486–491.
- [30] Valero, C. E. and Paulen, R. (2019b). Set-theoretic state estimation for multi-output systems using block and sequential approaches. In *2019 22nd International Conference on Process Control (PC19)*, pages 268–273. IEEE.
- [31] Vicino, A. and Zappa, G. (1996). Sequential approximation of feasible parameter sets for identification with set membership uncertainty. *IEEE Transactions on Automatic Control*, 41(6):774–785.
- [32] Villanueva, M. E., Houska, B., and Chachuat, B. (2015). Unified framework for the propagation of continuous-time enclosures for parametric nonlinear odes. *Journal of Global Optimization*, 62(3):575–613.
- [33] Wächter, A. and Biegler, L. T. (2006). On the implementation of an interior-point filter line-search algorithm for large-scale nonlinear programming. *Mathematical programming*, 106(1):25–57.